Pion-Nucleon Scattering Amplitudes in the Range 300–700 MeV

B. H. BRANSDEN AND P. J. O'DONNELL
Durham University, Durham, England

AND

R. G. MOORHOUSE
Rutherford Laboratory, Chilton, Didcot, Berkshire, England

(Received 5 April 1965)

The cross section for the scattering of π^+ and π^- by nucleons in the energy range 300–700 MeV has been analyzed in terms of energy-independent parameters. The parameterization is based on a dispersion relation satisfied by the partial-wave amplitudes, by replacing the left cut by a superposition of poles and the inelasticity function $R_l=\sigma_l(\text{tot})/\sigma_l(\text{el})$ by a ratio of polynomials in the momentum. Detailed results are presented for the real and imaginary parts of the phase shifts with $l\leqslant 3$. The structure of the "second resonance" is more complicated than has heretofore been thought, p_{11}, s_{11}, and d_{13} waves all playing an important part. The width of the d_{13} resonance is found to be considerably smaller than previous values from total cross-section measurements. The role of the (possibly resonant) amplitudes p_{11} and s_{11} is discussed.

1. INTRODUCTION

THE cross sections for the elastic scattering of pions by nucleons exhibit considerable structure over the whole energy range from threshold to 2 or 3 GeV. This structure has been interpreted in terms of the existence of resonant states. The analysis of the cross section in terms of partial waves, which allows the quantum numbers of the resonant states to be assigned, is complicated, except at the lowest energies, first by the number of partial waves concerned and secondly by the presence of a high degree of inelasticity. At present, because of these complications, many assignments of quantum numbers are in considerable doubt; but the existence of accurate data in several energy intervals and promise of a rapid accumulation of new data in the near future from experimental teams at Chilton, Saclay, and Berkeley makes it possible to hope that a phase-shift analysis without too much ambiguity can be achieved. The experimental situation is that not all three independent elements of the spin-density matrix are measured: differential cross sections have been measured to the order of 5% statistical accuracy; polarization, at fewer energies, to less accuracy; and the R parameter has not been measured at all. In this situation, taking account of statistical errors only, phase-shift analyses at one energy lead to a number of different solutions among which it is difficult to distinguish. In addition to statistical errors, there are unknown systematic errors, such as errors in normalization of the cross section, which can distort solutions. An example of overt systematic error is the well-known difference in total pion-nucleon cross-section measurements at Berkeley[1] and Saclay.[2] It is clear that if the experimental measurements considered as a function of energy contain systematic errors, then fitting the data at individual energies too closely without regard to the smoothness of the energy variation may result in distortions due to having fitted the noise as well as the signal.

The most promising way of reducing the number of solutions and in addition smoothly connecting the different solutions at different energies is to analyze the data over a range of energies simultaneously in terms of energy-independent parameters. Extensive and successful work based on these ideas in the case of nucleon-nucleon scattering has been reported by Stapp, Noyes, and Moravcsik.[3] In the pion-nucleon case such a program has only been reported by one other group,[4] in which the real and imaginary parts of the phase shifts are either expressed as polynomials in the momentum or in terms of Breit-Wigner forms. In the present work an entirely different method of parameterization is used, suggested by the analytic properties of the partial-wave scattering amplitudes. The first application of this parameterization has been to the energy interval from threshold to 700 MeV, covering the region of the "second resonance."[5]

In Sec. 2, notation is established and necessary formulas connecting the phase shifts and the various cross sections are collected for references. In Sec. 3, the general method of parameterization that we have adopted is given, while in Sec. 4 the choice of data and its normalization is discussed. The phase shifts in the

[1] T. J. Devlin, B. J. Moyer, and V. Perez-Mendez, Phys. Rev. **125**, 690 (1962).

[2] J. C. Brisson, J. F. Detoeuf, P. Falk-Vairant, L. van Rossum, and G. Valladas, Nuovo Cimento **19**, 210 (1961); P. Bareyre, G. Bricman, G. Valladas, G. Villet, J. Bizard, and J. Sequinot, Phys. Letters **8**, 137 (1964).

[3] H. P. Stapp, H. P. Noyes, and M. J. Moravcsik, in *Proceedings of the 1962 Annual International Conference on High Energy Physics at CERN*, edited by J. Prentki (CERN, Geneva, 1962), p. 131.

[4] B. T. Feld and L. D. Roper, in *Proceedings of the Sienna International Conference on Elementary Particles, 1963*, edited by G. Bernadini and G. P. Puppi (Società Italiana di Fisica, Bologna, 1963), Vol. 1, p. 400; L. D. Roper, Phys. Rev. Letters **12**, 340 (1964). L. D. Roper and R. M. Wright, University of California Radiation Laboratory Report No. 7846, 1964 (unpublished).

[5] Some preliminary results have been reported in B. H. Bransden, P. J. O'Donnell, and R. G. Moorhouse, Phys. Letters **11**, 339 (1964).

energy interval of interest, 300–700 MeV, must be connected with those at lower energies and this connection is exhibited in Sec. 5, while in Sec. 6 the actual searches carried out between 300 and 700 MeV are described in detail. A summary of our conclusions will be found in Sec. 7.

Future reports will describe further extensions of the energy range to cover first the region of the third resonance at 900 MeV and ultimately to the highest energies for which well defined resonances are observed.

2. NOTATION

In this section we define the partial-wave amplitudes and give the connection between these and the cross sections both to establish notation and for ease of reference.

The relations between the center-of-mass energy w, the pion laboratory energy T and the momentum $\mathbf{q}$ are[6]

$$w^2=(m+1)^2+2mT \tag{2.1}$$

and

$$q^2=[w^2-(m+1)^2][w^2-(m-1)^2](2w^2)^{-1}, \tag{2.2}$$

where m is the mass of the nucleon.

In the center-of-mass system the differential cross section can be written

$$\frac{d\sigma}{d\Omega}=\sum_{\text{spins}}\left|\left(f\left|f_1+\frac{(\boldsymbol{\sigma}\cdot\mathbf{q}_2)(\boldsymbol{\sigma}\cdot\mathbf{q}_1)}{q_1q_2}f_2\right|i\right)\right|^2, \tag{2.3}$$

where $\mathbf{q}_1$ ($\mathbf{q}_2$) denotes the initial (final) pion momentum, and the matrix element is taken between two component spinors.

The amplitudes f_1 and f_2 are related to the phase shifts in the appropriate eigenstate of isotopic spin by

$$f_1=\sum_{l=0}^{\infty}f_{l+}P_{l+1}'(x)-\sum_{l=2}^{\infty}f_{l-}P_{l-1}'(x), \tag{2.4}$$

and

$$f_2=\sum_{l=1}^{\infty}(f_{l-}-f_{l+})P_l'(x), \tag{2.5}$$

where

$$x=\cos\theta \tag{2.6}$$

and

$$f_{l\pm}=q^{-1}\exp(i\delta_{l\pm})\sin\delta_{l\pm}. \tag{2.7}$$

When $\delta_{l\pm}$ is complex we write Eq. (2.7) explicitly as

$$f_{l\pm}=(2iq)^{-1}[\exp(-2\beta_{l\pm}+2i\alpha_{l\pm})-1], \tag{2.8}$$

$$=(2iq)^{-1}[\eta_{l\pm}\exp(2i\alpha_{l\pm})-1], \tag{2.9}$$

where

$$\delta_{l\pm}=\alpha_{l\pm}+i\beta_{l\pm}. \tag{2.10}$$

The differential cross section (2.3) becomes, on summing over spins,

$$d\sigma/d\Omega=|f(\theta)|^2+|g(\theta)|^2, \tag{2.11}$$

where the no-flip amplitude $f(\theta)$ and the spin-flip amplitude $g(\theta)$ are given by

$$f(\theta)=f_1(\theta)+\cos\theta f_2(\theta), \tag{2.12}$$

and

$$ig(\theta)=\sin\theta f_2(\theta). \tag{2.13}$$

The polarization $P(\theta)$ of the final nucleon spin is defined as

$$(d\sigma/d\Omega)P(\theta)=2[\mathrm{Re}f(\theta)g^*(\theta)]\sin\theta. \tag{2.14}$$

The amplitudes for π^-p scattering and charge exchange are obtained from those for the pure isospin channels $T=\frac{3}{2}$ and $T=\frac{1}{2}$.

For $\pi^-+p\rightarrow\pi^-+p$, the combination of the f_i^T is

$$\tfrac{1}{3}(f_i^{3/2}+2f_i^{1/2}), \quad i=1,2 \tag{2.15}$$

and for $\pi^-+p\rightarrow\pi^0+n$, is

$$(\tfrac{1}{3}\sqrt{2})(f_i^{3/2}-f_i^{1/2}), \quad i=1,2. \tag{2.16}$$

If we write

$$\zeta_{l\pm}=\exp(2i\delta_{l\pm}), \tag{2.17}$$

then the total cross section $\sigma_{l\pm}$ and the elastic cross section $\sigma_{l\pm}(\mathrm{el})$ for the $l\pm$ partial waves are given by

$$\sigma_{l\pm}=(2\pi/q^2)(j+\tfrac{1}{2})(1-\mathrm{Re}\zeta_{l\pm}), \tag{2.18}$$

and

$$\sigma_{l\pm}(\mathrm{el})=(\pi/q^2)(j+\tfrac{1}{2})|1-\zeta_{l\pm}|^2, \quad j=(l\pm\tfrac{1}{2}). \tag{2.19}$$

The inelasticity coefficient $R_{l\pm}$ is related to σ_l and $\sigma_l(\mathrm{el})$ by the optical theorem

$$R_{l\pm}\equiv\frac{\sigma_{l\pm}}{\sigma_{l\pm}(\mathrm{el})}=\frac{\mathrm{Im}(f_{l\pm})}{q|f_{l\pm}|^2}, \tag{2.20}$$

so that $R_{l\pm}\geqslant 1$.

In the analysis of pion-proton experimental scattering data a modification has to be introduced to take into account the effects of Coulomb scattering. For the energy range, we consider in this paper the separation of Coulomb and nuclear effects that have been achieved by using the results of Solmitz.[7]

In this approximation, an amplitude for Coulomb scattering correct to first order in $\alpha=(e^2/\hbar c)$ is added to the nuclear amplitudes $f(\theta)$ and $g(\theta)$. Explicitly,

$$\bar{f}(\theta)=f_c(\theta)+f(\theta),$$
$$\bar{g}(\theta)=g_c(\theta)+g(\theta), \tag{2.21}$$

where

$$f_c(\theta)=\mp e^2(2q(v_\pi+v_p)\sin^2\tfrac{1}{2}\theta)^{-1}\times[1+\tfrac{1}{2}v_\pi v_p(1+\cos\theta)-\tfrac{1}{4}v_p^2(2\mu_p-1)\times(1-\cos\theta)] \tag{2.22}$$

and

$$g_c(\theta)=\pm e^2(2q(v_\pi+v_p)\sin^2(\tfrac{1}{2}\theta))^{-1}\times[\tfrac{1}{2}\mu_p v_\pi v_p+\tfrac{1}{4}v_p^2(2\mu_p-1)]\sin\theta.$$

[6] Natural units with $m_\pi=c=\hbar=1$ are used.

[7] F. T. Solmitz, Phys. Rev. **94**, 1799 (1950).

In these expressions, v_π and v_p are the pion and proton velocities in the center-of-mass system and μ_p is the magnetic moment of the proton in nuclear magnetons. At low energies, nuclear and Coulomb scattering can no longer be separated accurately in this way,[8] but at 300 MeV, our lowest energy, the error arising from the approximations of Eqs. (2.21) and (2.22) is negligible.

3. PARAMETERIZATION—GENERAL PROPERTIES

In making an analysis of experimental data at many energies simultaneously, the energy dependence of the partial-wave amplitude poses a problem, especially if, as in the pion-nucleon case, the scattering process soon becomes very inelastic as the energy is increased. Our method has been to make use of the analytic properties of the partial-wave scattering amplitude and, in particular, to make use of the unitarity relation at physical energies, between the imaginary part of the inverse of $f_{l\pm}$ and the inelasticity coefficient $R_{l\pm}$, viz,

$$\mathrm{Im}f_{l\pm}^{-1}=-qR_{l\pm}(q). \tag{3.1}$$

Our parameterization scheme will be based on this equation and on the following dispersion relation[9] for $\mathrm{Re}f_{l\pm}^{-1}$:

$$\mathrm{Re}f_{l\pm}^{-1}(q)=-\frac{(q^2-q_0^2)}{\pi}\int_0^\infty dx^2\frac{xR_{l\pm}(x)}{(x^2-q^2)(x^2-q_0^2)}+\frac{(q^2-q_0^2)}{\pi}\int_{-\infty}^{-a}dx^2\frac{\Delta f_{l\pm}^{-1}(x)}{(x^2-q^2)(x^2-q_0^2)}+\sum_{n=0}^{l}\lambda_n/q^{2n}, \tag{3.2}$$

where

$$a=(1-1/4m^2)/(1+1/2m^2) \tag{3.3}$$

and the λ_n are constants. $\Delta f_{l\pm}^{-1}$ denotes the discontinuity of $-2if_{l\pm}^{-1}$ across the left-hand cut. For those cases in which the amplitude has a zero for physical values of energy additional poles may be added to the right-hand side of Eq. (3.2) for otherwise the expression is too restrictive.

Since in the great majority of our searches for solutions we are concerned with energies which are well away from the threshold region, we consider delta functions for $\Delta f_{l\pm}^{-1}$ to be a reasonable form of parameterization and accordingly set

$$\Delta f_{l\pm}^{-1}=\sum_{n=1}^{K} r_{l\pm}{}^n\delta(q^2+q_n{}^2), \tag{3.4}$$

where $r_{l\pm}{}^n$ and $q_n{}^2$ are our parametric constants. The value of K may be different for different l since for a given energy the number of poles needed increases as we describe lower angular momentum states. Apart from this consideration, there does not exist any *a priori* method of fixing the value of K. This choice of parameterization which replaces the left cut by a series of poles has found many applications, but in dealing with $R_{l\pm}$ on the right no such standard technique is available. Any parametric form chosen for this function must be of a sufficiently flexible form to allow quite different kinds of behavior to take place, since the inelasticity coefficient is virtually an unknown function. In the absence of any real knowledge about the behavior of $R_{l\pm}$, we have considered the ratio of polynomials, whose energy-independent constants are taken to be the parameters, to be a suitable form. The polynomials were chosen in such a way as to help keep computing time at a minimum while retaining the flexibility noted above. In our searches we used particular cases of the following general expression:

$$R_{l\pm}(q)=1+\theta(q-q_1)\left\{a_{l\pm}\frac{q(q-q_1)}{(1+q^2/A^2)}+b_{l\pm}\frac{(q-q_1)}{(1+q^2/B^2)}\right\}+\theta(q-q_2)\left\{c_{l\pm}\frac{q(q-q_2)}{(1+q^2/C^2)}+\delta_{l,0}d_{l\pm}\frac{q(q^2-q_2^2)^{1/2}}{(1+q^2/D^2)}\right\}, \tag{3.5}$$

where $a_{l\pm}$, $b_{l\pm}$, $c_{l\pm}$, $d_{l\pm}$, A, B, C, and D are constants, q_1 is the first inelastic threshold, and q_2 is the threshold for η production. This form allowed analytic expressions to be derived for the integral in Eq. (3.2).

This form of $R_{l\pm}(q)$ does not exhibit the correct behavior at each inelastic threshold, and indeed there are many inelastic thresholds in our energy range, but the threshold dependence holds only over a small energy where, most probably, the contribution of the new process to the reaction cross section is completely unimportant. The only exception to this in our energy range appears to be in the $T=\frac{1}{2}$ s wave at the η-production threshold. For this state we have introduced the last term in Eq. (3.5), which has the correct behavior at this threshold. The parameterization of the inelasticity is discussed further in Sec. 6.

4. DATA FITTING

A list of all the experimental data used is given in Appendix A. As explained in later sections the results of analysis of low-energy data (energy less than 98 MeV) by Hamilton and Woolcock[10] were taken into account in determining the s and p scattering lengths.

Above 310 MeV most of the data used are the recent

[8] N. F. Mott and H. S. W. Massey, *Theory of Atomic Collisions* (Oxford University Press, London, 1948), p. 302. See also Ref. 10.

[9] J. W. Moffat, Phys. Rev. **121**, 926 (1961).

[10] J. Hamilton and W. S. Woolcock, Rev. Mod. Phys. **35**, 237 (1963).

differential-cross-section (and polarization) data from experiments at Berkeley and Saclay.[11] Older experiments of low accuracy were omitted; we did not make use of experiments where the results were presented solely as coefficients in a $\cos\theta$ expansion.

Having adopted these general criteria we attempted no further selection of data. In particular we did not exclude individual data points, as this might have introduced an unwarranted subjective element into the analysis. Where the authors of an experiment have given a forward point involving a dispersion relation calculation, we have included it.

As explained in Secs. 2 and 3, the cross sections and polarizations at the energies and angles for which experiments exist can be calculated in terms of certain parameters. We then form the sum

$$M=(N-n)^{-1}\sum_{i=1}^{N}((O_i-C_i)^2/\Delta_i^2), \tag{4.1}$$

where O_i and Δ_i are the observed quantity and error, respectively, and C_i is the corresponding calculated quantity. N is the number of data points and n the number of independent parameters. The best values of the parameters are now found by minimizing M.

This formulation, while used in most of our fits, does not take account of normalization errors in the data. One standard method of doing this is to have a normalization parameter for each complete differential cross-section experiment. Unfortunately, this would introduce too many extra parameters and lead to excessive computing time. In some runs an attempt to compensate for possible "common errors" in the data was made following a method due to Davidon,[12] which replaces Eq. (4.1) by the more general form.

$$M=\frac{1}{(N-n)}\sum_{i,j}^{N}H_{ij}\frac{(O_i-C_i)}{\Delta_i}\frac{(O_j-C_j)}{\Delta_j}, \tag{4.2}$$

where

$$H_{ij}=\delta_{ij}-\left(\frac{\epsilon_i}{\Delta_i}\right)\left(\frac{\epsilon_j}{\Delta_j}\right)\left[I+\sum_k\left(\frac{\epsilon_k}{\Delta_k}\right)^2\right]^{-1}. \tag{4.3}$$

This expression takes into account the possibility of common errors ϵ_i with the result that off-diagonal elements do not necessarily vanish as in Eq. (4.1). Experience has shown that the fits obtained using either method are not significantly different, so that in the future we propose to use merely the simpler Eq. (4.1).

To find the parameters pertaining to the $T=\frac{3}{2}$ amplitude it is sufficient to fit the π^+p data. Having thus fixed best values of these amplitudes we use them, along with the still variable $T=\frac{1}{2}$ amplitudes, to calculate the C_i for the π^-p data. The $T=\frac{1}{2}$ parameters and amplitudes are then found by minimizing M for the π^-p data. The whole process may be performed repeatedly to find many possible sets of $T=\frac{3}{2}$, $T=\frac{1}{2}$ solutions, out of which the best are selected with reference to the relative M values.

5. PHASE SHIFTS AT AND BELOW 300 MeV

There is a natural boundary zone in pion-nucleon scattering from 250 to 350 MeV; for below 250 MeV inelasticity can be neglected and pion-nucleon scattering analyzed using real phase shifts only, while at 350 MeV, inelasticity is already important and analysis in terms of real phase shifts only is no longer possible. With the consequent proliferation of parameters above this energy, it is important to use a method such as ours, or information from the peripheral pion-nucleon interactions, or both, in order to limit the number of solutions. In conducting our searches above this energy zone we could in principle proceed with no *a priori* information from within or below it. But our task is simplified if we can take some already known phase shifts within the zone as approximate boundary values in our searches, and it is fortunate that there are recent $\pi^\pm p$ scattering experiments[13,14] at 310 MeV accompanied by extensive phase-shift analyses.[15,16]

Foote *et al.*[15] have analyzed $\pi^\pm p$ data at 310 MeV, and, on the basis of their results, Vik and Rugge[16] have fitted π^+p and π^-p differential cross sections, polarization, total cross section, inelastic cross section, and charge-exchange differential cross section (this latter from an experiment[17] at 317 MeV). Phase shifts up to f waves were included and the three final Vik-Rugge solutions are shown in Table I; *spdf* I is the best fit while *spdf* II is somewhat better than *spdf* III.

However, doubts have been cast[18] on the stability of the method when f waves are included; it could be that there exist not only these three, but many more, solutions with a χ^2 of the same order. Kane and Spearman[18] have attempted to resolve this possible dilemma in the following way. From an analysis[19] of low-energy pion-nucleon scattering they are able to obtain the long-range forces acting on the pion-nucleon system, in the form of the branch-cut discontinuities nearest to the physical region in the $\cos\theta$ plane of the invariant amplitudes. The higher partial waves can then be obtained from these nearby discontinuities (that is, long-range forces) and 310 MeV is a low enough energy for

[11] See Appendix A for references.
[12] See U. E. Kruse and R. C. Arnold, Phys. Rev. **116**, 1008 (1959).
[13] E. H. Rogers, O. Chamberlain, J. Foote, H. Steiner, C. Weigand, and T. Ypsilantis, Rev. Mod. Phys. **33**, 356 (1961); J. Foote, O. Chamberlain, E. Rogers, H. Steiner, C. Weigand, and T. Ypsilantis, Phys. Rev. **122**, 948 (1961).
[14] H. R. Rugge and O. T. Vik, Phys. Rev. **129**, 2300 (1963).
[15] J. Foote, O. Chamberlain, E. Rogers and H. Steiner, Phys. Rev. **122**, 959 (1961).
[16] O. T. Vik and H. R. Rugge, Phys. Rev. **129**, 2311 (1963).
[17] J. C. Carris, R. W. Kenney, V. Perez-Mendez, and W. R. Perkins, Phys. Rev. **121**, 893 (1961).
[18] G. L. Kane and T. D. Spearman, Phys. Rev. Letters **11**, 45 (1963).
[19] T. D. Spearman, Phys. Rev. **129**, 1847 (1963).

TABLE I. The *spdf* solutions of Vik and Rugge, Ref. 16, at 310 MeV. δ is the real part of the phase shift in degrees; η is the inelasticity parameter.

	$s_{3,1}$	$p_{3,1}$	$p_{3,3}$	$d_{3,3}$	$d_{3,5}$	$f_{3,5}$	$f_{3,7}$	$s_{1,1}$	$p_{1,1}$	$p_{1,3}$	$d_{1,3}$	$d_{1,5}$	$f_{1,5}$	$f_{1,7}$
I δ	−14.9	+0.4	135.1	5.1	−6.5	0.8	−1.8	−5.9	−5.5	1.7	−5.5	15.3	−0.1	2.3
η	1.00	1.00	1.00	1.00	1.00	1.00	1.00	1.00	1.00	0.99	0.99	1.00	1.00	1.00
II δ	−21.1	−11.8	137.0	−3.1	1.2	−1.7	3.1	10.9	23.0	−3.6	5.9	0.3	1.8	−0.7
η	1.00	1.00	1.00	1.00	1.00	1.00	1.00	1.00	0.94	1.00	1.00	1.00	1.00	1.00
III δ	−15.4	−0.4	135.6	4.4	−6.2	0.7	−1.4	3.7	26.4	8.6	−0.3	3.1	0.6	−0.1
η	1.00	1.00	1.00	1.00	1.00	1.00	1.00	1.00	1.00	0.98	1.00	1.00	1.00	1.00

the f waves to count as "higher partial waves" and to be obtained in this way. With the calculated f waves a search can be made for a fit to the data varying the s, p, and d waves only. So far the results have only been published for the π^+p, $T=\frac{3}{2}$, state and are given in the first row of Table II, labeled KS.

Donnachie, Hamilton, and Lea[20] have made a similar calculation predicting p, d, and f waves (with the exception of p_{11}) up to 400 MeV. Again they take the long-range, or peripheral interaction, from phenomenological studies[21] in pion-nucleon dispersion relation but in calculating the p, d, and f waves they use partial-wave dispersion relations rather than the fixed-energy dispersion relation used by Kane and Spearman. Their results at 310 MeV are to be found in the second row of Table II, labeled DHL.

It is evident that both these calculations strikingly disagree with the solution *spdf* I and *spdf* III of Vik and Rugge, but are in fair over-all agreement with *spdf* II. The agreement is particularly good for the calculations of Donnachie, Hamilton, and Lea (as these authors have remarked), except for d_{35} and the magnitude of the f waves. Thus from the peripheral interaction work a solution at 310 MeV with the general characteristics of *spdf* II is strongly indicated. As a note of caution it may be said that the two peripheral interaction calculations under discussion are not totally independent, as both are based on the same type of method[22] for extracting the peripheral interaction from pion-nucleon scattering.

It should be remarked that *spdf* II is the only Vik-Rugge solution with inelasticity in a $T=\frac{1}{2}$, $J=\frac{1}{2}$ state, which appears to be required by other analyses.[23,24]

A fit by the present authors to π^+p data in the range 100 to 350 MeV also gave support to the general correctness of *spdf* II. This search for a fit was performed mainly as a test for the viability of our method and was subject to the following restrictions;

(i) As a lower boundary condition, the s and p scattering lengths were fixed to the values given by Hamilton and Woolcock.[10]

(ii) The d waves (d_{33} and d_{35}) were restricted by the negative as indicated by the peripheral interaction work of Donnachie, Hamilton, and Lea.[20]

(iii) The p_{33} phase shift was forced to pass through 90° at 200 MeV. Under these conditions the amplitudes were expressed as a function of a total of 10 parameters, 1 in each of the d and f amplitudes and 2 in each of the s and p amplitudes.

Starting from zero values of the parameter, one search for a minimum yielded a reasonable fit to the data. In particular it was found that the pole positions and residues of the p_{33} inverse amplitude have adjusted themselves so as to yield the p_{33} amplitude in essentially the Layson[25] generalized Breit-Wigner form:

$$\frac{2m\gamma_L a}{(q_R^2-q^2)(1+(q^2a^2)^{-1})-2m\gamma_L iqa}$$

where m is the mass of the nucleon and q_R is the momentum at resonance. With resonance at 205 MeV, Layson's values were[25] $a=0.714$, $\gamma_L=0.133$; our values with resonance at 200 MeV were $a=0.707$, $\gamma_L=0.127$. The phase shifts at 310 MeV are given in the third row of Table II, labeled BMO, and agree very well with the *spdf* II solution of Vik and Rugge. It may particularly be noted that the d_{35} phase shift, which is constrained to be negative, is, at 0°, as close as it can get to the 1.2° of *spdf* II; and that the f waves agree in sign with both the results of Donnachie, Hamilton, and Lea and *spdf* II, and in magnitude with *spdf* II.

These results could be taken as further support for a solution at 310 MeV of the type *spdf* II. However, in view of the constraints, and the fact that there was only one search, the skeptical reader might consider that the result was partly forced and for the rest coincidental. We do not think that there is any force in the objection on the grounds of constraints; constraints (i) operate

[20] A. Donnachie, J. Hamilton, and A. T. Lea, Phys. Rev. **135**, B515 (1964).

[21] J. Hamilton, P. Menotti, G. C. Oades, and L. L. J. Vick, Phys. Rev. **128**, 1881 (1962); J. Hamilton, *Proceedings of the 1963 Scottish Universities Summer School in Strong Interactions and High Energy Physics* (Oliver and Boyd, London, 1964), p. 281.

[22] J. Hamilton, P. Menotti, and T. D. Spearman, Ann. Phys. (N. Y.) **12**, 172 (1961); J. Hamilton, P. Menotti, T. D. Spearman, and W. S. Woolcock, Nuovo Cimento, **20**, 519 (1961); J. Hamilton, T. D. Spearman, and W. S. Woolcock, Ann. Phys. (N. Y.) **17**, 1 (1962); and Refs. 10 and 21.

[23] P. Bareyre, C. Bricman, G. Valladas, G. Villet, J. Bizard, and J. Sequinot, Phys. Letters **8**, 137 (1964).

[24] P. Auvil and C. A. Lovelace, Nuovo Cimento **33**, 473 (1963).

[25] W. M. Layson, Nuovo Cimento **20**, 1207 (1961).

TABLE II. Phase shifts at 310 MeV.[a]

	Phase shifts in degrees												
	$s_{3,1}$	$p_{3,1}$	$p_{3,3}$	$d_{3,3}$	$d_{3,5}$	$f_{3,5}$	$f_{3,7}$	$s_{1,1}$	$p_{1,1}$	$p_{1,3}$	$d_{1,3}$	$d_{1,5}$	$f_{1,5}$	$f_{1,7}$
KS, δ	−19.5	−6.3	134.4	1.0	−3.1	−0.04	0.49							
DHL, δ		−13.0	137.4	−1.3	−2.1	−0.1	−0.6			−3.5	5.7	0.7	0.8	−0.1
BMO, δ	−20.52	−13.5	135.9	−2.6	0.0	−0.1	3.2							

[a] KS–results of Kane and Spearman, Ref. 18; DHL–results of Donnachie, Hamilton and Lea, Ref. 20; BMO–results of preliminary ten-parameter searches over energy range 100–350 MeV discussed in Sec. 5.

strongly at the lower energies (~100 MeV) only, and are designed to provide a smooth join to pion-nucleon scattering below 100 MeV; constraints (ii) operate one for and one against *spdf* II; constraint (iii) must be (nearly) obeyed by any correct result and is not so much a constraint as an aid to quick solutions.

Nevertheless, we ourselves prefer to invert the force of the argument, considering that *spdf* II has already been chosen as the correct type of solution. So given already the correctness of the type *spdf* II, the result of the search from 100 to 350 MeV shows that our method, provided additionally with lower boundary conditions and the fact of resonance in one partial wave, is likely to produce the correct solution.

6. PION-NUCLEON AMPLITUDES: 300 TO 700 MeV

A. Form of Parameterization

To use in our searches (for pion-nucleon scattering amplitudes between 300 and 700 MeV) we obtained in Sec. 3 a rather general analytic parameterization. The least physically possible number of parameters is large (with consequent long computing time involved in search for a minimum value of M), so that we used all available information to minimize the number of parameters and limit their range of variation. Three general limitations were imposed on the parameterization:

(i) In the last section we gave reasons for believing that the *spdf* II solution of Vik and Rugge is substantially correct. Consequently, in the range 300–700 MeV, we principally searched on those parameterizations, and those regions in the subsequent parameter space, which, at 310 MeV, give rough agreement with *spdf* II (and also represent a reasonably smooth combination of our own fit to the π-N experiments from 0 to 300 MeV). This is not regarded as a strict limitation on our searches and we have performed one or two searches which do not conform to this condition.

(ii) It seems likely[26] that the d_{13} wave resonates near 600 MeV at the "second resonance." Our parameterizations, with one exception, have maintained a d_{13} resonance between 550 and 650 MeV with the exact position and the width being determined by the search for the minimum of M, that is by the fit to the experiments.

(iii) It is a reasonable physical assumption that, for a given partial wave, the energies for which inelastic scattering is important are greater that those for which elastic scattering dominates. We have assumed that there is no $T=\frac{3}{2}$ f-wave inelasticity up to 700 MeV; this assumption, while probably never too far wrong, is open to question between 600 and 700 MeV.

These are the general limitations imposed on the parameterization. However, there are more particular limitations, which may vary somewhat from one search to another, and whose object is to obtain the maximum physically reasonable variation in each partial wave for the minimum number of parameters. Consider first $\sigma_{\text{tot}}/\sigma_{\text{el}}$ which as described in Sec. 3 is parameterized as

$$R_{l\pm}(q)=1+\theta(q-q_1)\left\{a_{l\pm}\frac{q(q-q_1)}{(1+q^2/A^2)}+b_{l\pm}\frac{(q-q_1)}{(1+q^2/B^2)}\right\}$$
$$+\theta(q-q_2)\left\{c_{l\pm}\frac{q(q-q_2)}{(1+q^2/C^2)}+\delta_{l,0}d_{l\pm}\frac{q(q^2-q_2^2)^{1/2}}{(1+q^2/D^2)}\right\},$$

where q_1 is the first inelastic threshold and q_2 the threshold for η production. $a_{l\pm}$, $b_{l\pm}$, $c_{l\pm}$, $d_{l\pm}$ are variable parameters in each search while (so that the search program does not require the computer to calculate a complicated expression very many times) A, B, C, and D are the same for each partial wave and fixed at the beginning of each search. A-, C-, and D-type inelasticities each rise to an asymptotic maximum (approximately attained for $q\gg A$, C or D) while the B type rises to a maximum at q greater than $2q_1$, (which corresponds to about 530 MeV), the exact position depending on the magnitude of B. It is of course important to remember, now and later, that the behavior of $\eta_{l\pm}$ is not like that of $R_{l\pm}$. In particular, R is likely to remain constant or slowly varying over a resonance, while η may exhibit a sharp minimum at that point. Now, with this general parameterization, for all d and f waves except the d_{13}, one type of inelasticity, either A type or C type, was chosen; for the lower waves two types of inelasticity were allowed.

Secondly, consider the rest of the parameterization which consists of the winding-point parameters λ_n [see Eq. (3.2)] and the residues and positions of the left-

[26] R. Omnes and G. Valladas, *Proceedings of the Aix-en-Provence International Conference on Elementary Particles, 1961* (Centre d'Etudes Nucleaires de Saclay, Siene et Oise, 1961), Vol. 1, p. 467.

hand poles. The coefficient λ_l of the *leading* winding-point singularity is just the inverse scattering length for that partial wave. For the s and p waves these parameters were either fixed at the values given by Hamilton and Woolcock[10] or allowed to vary somewhat from them. In all partial waves the *nonleading* winding-point parameters were almost always put equal to zero and not varied. Usually, the left-hand singularities were

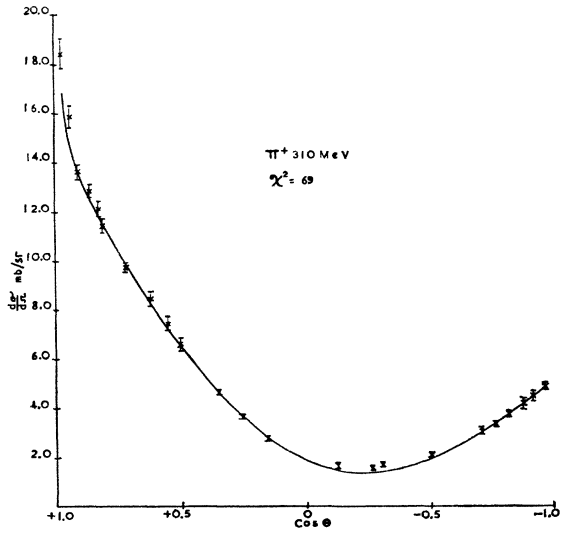

FIG. 1. The fit of solution 1 to the $\pi^{\pm}$-p differential cross section.

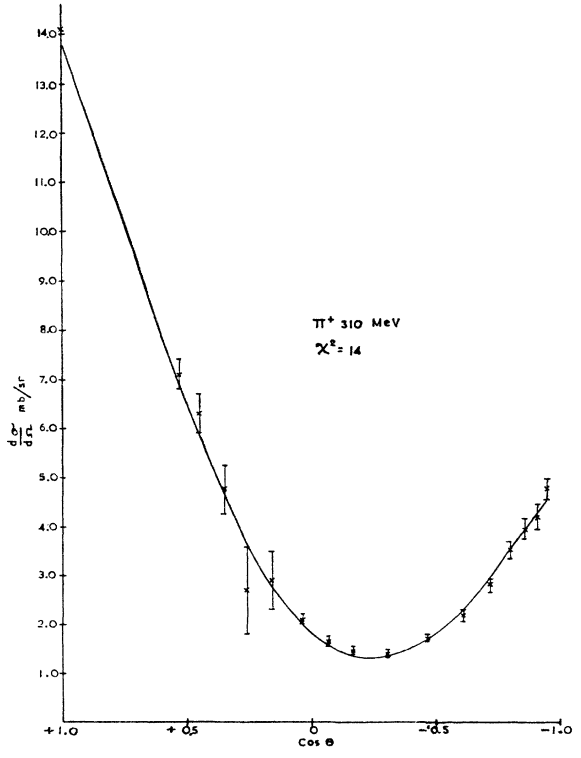

FIG. 2. The fit of solution 1 to the $\pi^{\pm}$-p differential cross section.

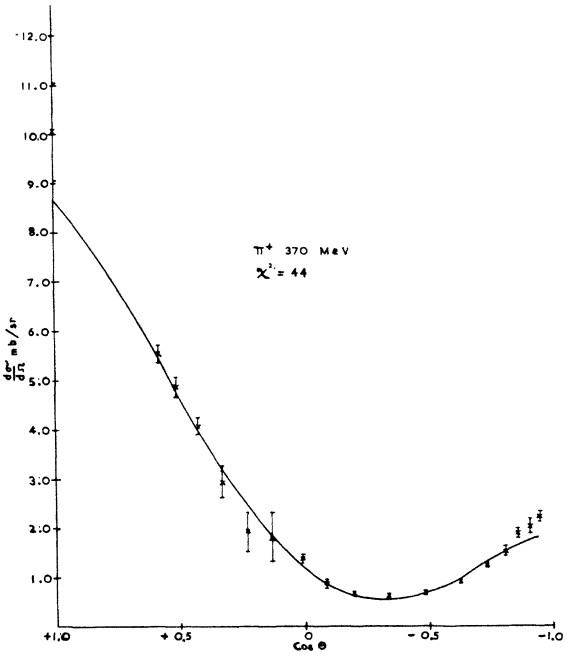

FIG. 3. The fit of solution 1 to the $\pi^{\pm}$-p differential cross section.

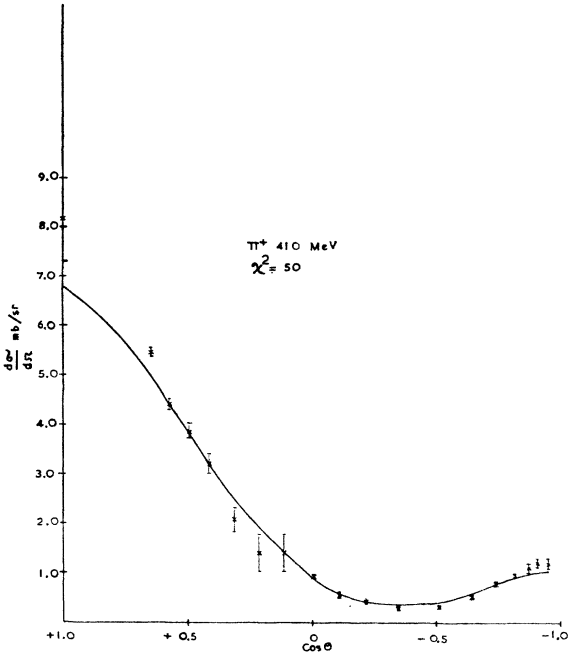

FIG. 4. The fit of solution 1 to the $\pi^{\pm}$-p differential cross section.

represented by two poles of *fixed position*, one at $q^2 \simeq -1$ and the other at $q^2 \simeq -20$ (units of pion mass) and *variable residue*. In some partial waves, for example, the p_{33} amplitude, more poles were necessary. In all partial waves the pole positions were regarded as potentially variable, and in some searches actually varied.

We give in Appendix B the form of the partial-wave

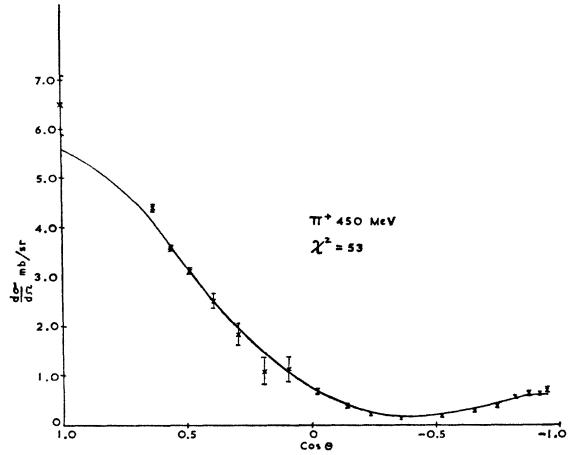

FIG. 5. The fit of solution 1 to the $\pi^{\pm}$-p differential cross section.

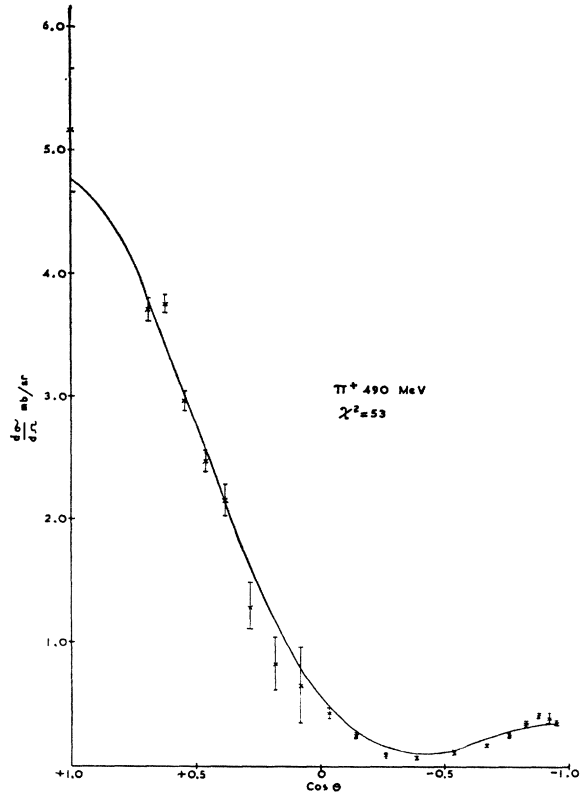

FIG. 6. The fit of solution 1 to the $\pi^{\pm}$-p differential cross section.

amplitude that appeared in our computing program together with the particular application of it in the search that led to solution 1, described below. It should be emphasized that even with the limitations described above, our method of parameterization was capable of giving very different types of energy-dependent behavior. In particular a resonance in a partial wave (either pure or of the type background and resonance) does not need any special form of the partial-wave amplitude.

B. Solutions

As explained in Sec. 4, our procedure is first to determine the $T=\frac{3}{2}$ amplitudes by a fit to the π^{+}-p data and then to use these $T=\frac{3}{2}$ amplitudes in a determination of the $T=\frac{1}{2}$ amplitudes by a fit to the π^{-}-p data. Two solutions (I, I′) have already been described[5,27];

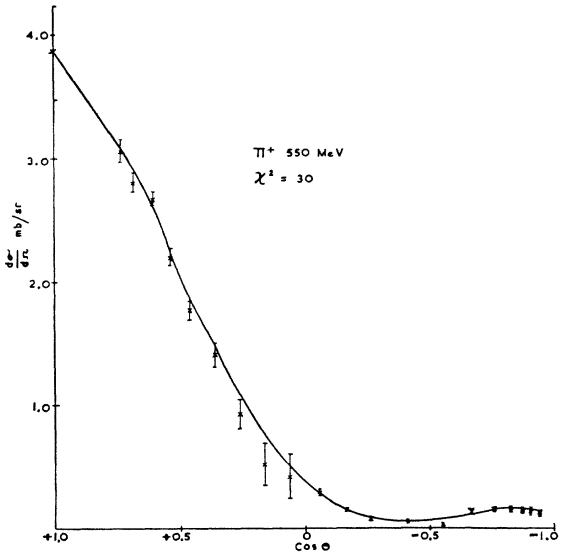

FIG. 7. The fit of solution 1 to the $\pi^{\pm}$-p differential cross section.

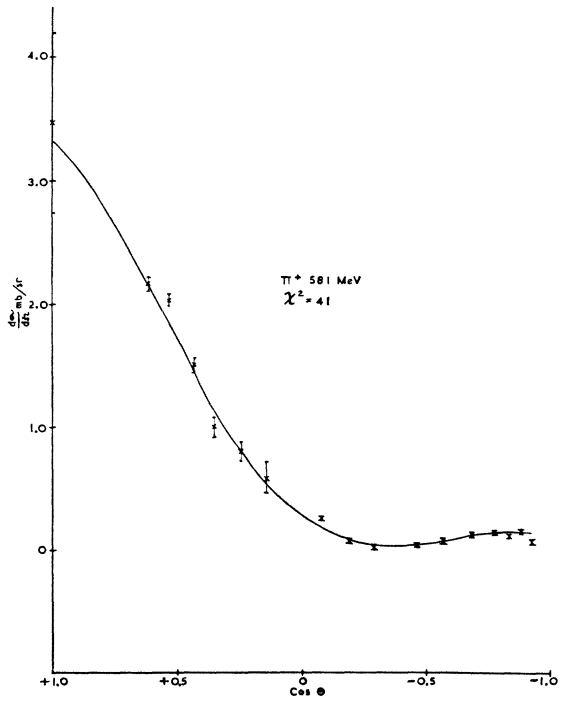

FIG. 8. The fit of solution 1 to the $\pi^{\pm}$-p differential cross section.

[27] B. H. Bransden, R. G. Moorhouse, and P. J. O'Donnell, Rutherford Laboratory Report No. NIRL/R/79 (unpublished).

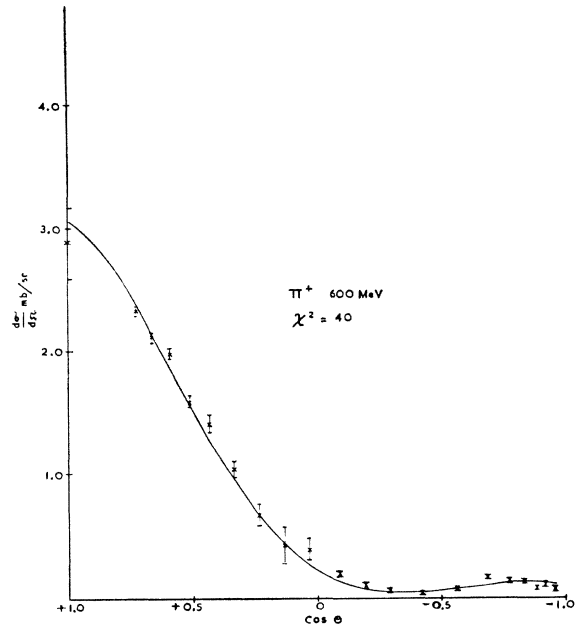

FIG. 9. The fit of solution 1 to the $\pi^{\pm}$-p differential cross section.

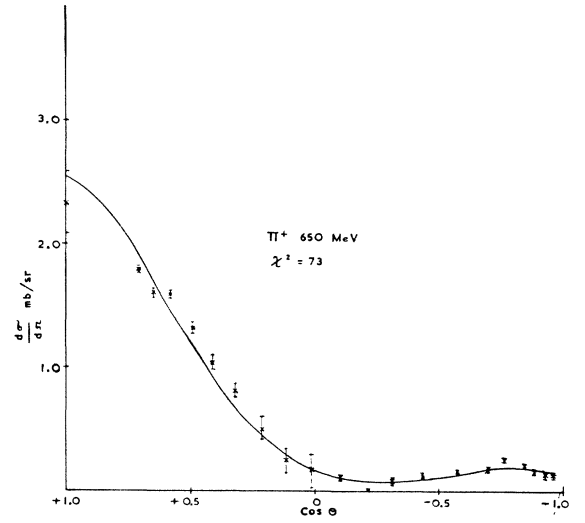

FIG. 10. The fit of solution 1 to the $\pi^{\pm}$-p differential cross section.

these solutions have been superseded by solutions 1 and 2 which contain a term in the s-wave inelasticity (term "d") with correct behavior at the threshold. Solution 1 corresponds to the old solution I and solution 2 to the old solution I′. The fit to the experimental data for solution 1 is shown in Figs. 1–33. The fit to the π^--p total cross sections is particularly interesting since there are only 5 π^--p total cross sections in the data to be fitted (out of a total of 396 data for the determination of the $T=\frac{1}{2}$ amplitudes). This means that they have negligible weight and that our π^--p total cross section is predicated from the assumptions of our method and the differential cross section only, so that the good agreement with the Saclay total-cross-section measurements[23] is noteworthy.

The phases, $\delta_{l\pm}{}^T$, and absorption parameters, $\eta_{l\pm}{}^T$, for solutions 1 and 2 are shown in Figs. 34–37 and Tables III and IV. The $T=\frac{3}{2}$ solution 2 is just a small perturbation of the $T=\frac{3}{2}$ solution 1, but the two solutions for $T=\frac{1}{2}$ apparently differ strikingly in the s wave. In solution 2 the real part of the s_{11} phase shift goes through $\frac{1}{2}\pi$, but in solution 1 it does not. This and other aspects of solutions 1 and 2 are discussed and compared in Sec. 7 below.

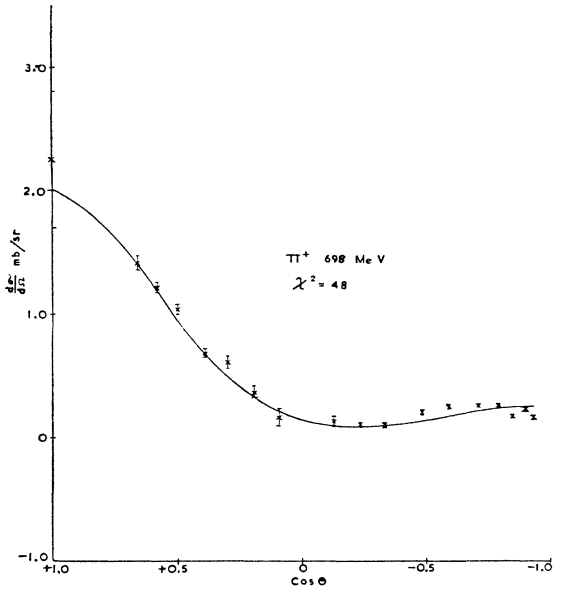

FIG. 11. The fit of solution 1 to the $\pi^{\pm}$-p differential cross section.

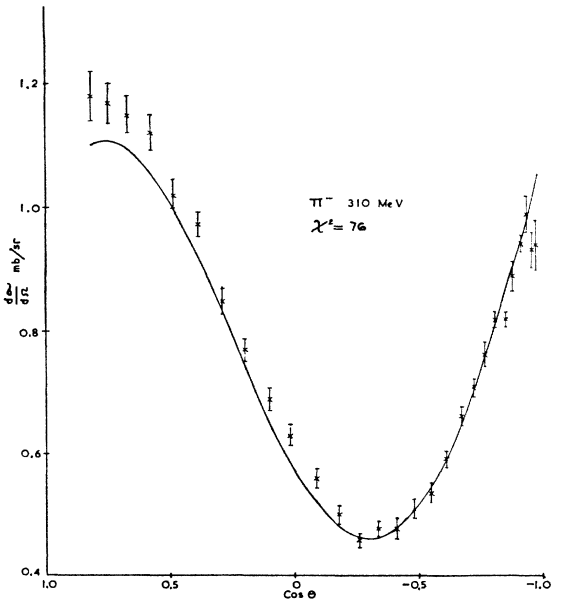

FIG. 12. The fit of solution 1 to the $\pi^{\pm}$-p differential cross section.

TABLE III. Solutions 1 and 2 for states with $T=\frac{1}{2}$.[a]

Energy (MeV)		310	370	410	450	490	533	572	600	650	698
s_{11} δ	1	9.3	10.9	12.4	14.5	17.8	24.7	37.9	39.6	27.0	−1.6
	2	10.9	12.7	14.5	17.1	21.4	30.3	48.2	63.7	127.7	147.8
η	1	0.998	0.995	0.992	0.987	0.978	0.953	0.657	0.428	0.159	0.186
	2	0.985	0.977	0.970	0.957	0.935	0.877	0.591	0.336	0.276	0.520
p_{13} δ	1	−6.0	−6.5	−6.8	−7.2	−7.3	−7.4	−7.6	−7.7	−7.8	−7.9
	2	−5.4	6.8	−7.8	−8.8	−10.0	−11.4	−12.8	−13.8	−16.1	−18.8
η	1	0.983	0.969	0.950	0.947	0.934	0.919	0.903	0.889	0.861	0.822
	2	0.997	0.993	0.988	0.981	0.972	0.959	0.942	0.927	0.890	0.837
p_{11} δ	1	16.9	34.7	46.2	55.2	61.8	64.3	64.2	62.3	56.3	48.5
	2	19.42	36.38	45.1	50.7	53.3	53.4	51.5	49.4	44.6	39.4
η	1	0.952	0.767	0.559	0.461	0.365	0.297	0.259	0.241	0.236	0.267
	2	0.296	0.725	0.584	0.480	0.410	0.364	0.342	0.338	0.351	0.393
d_{15} δ	1	−0.29	0.53	0.74	1.0	1.4	1.9	2.7	3.5	5.7	10.8
	2	0.4	0.63	0.9	1.3	1.8	2.4	3.4	4.3	6.8	11.7
η	1	1	1	1	1	1	1	1	1	1	1
	2	1	1	1	1	0.999	0.997	0.994	0.990	0.975	0.928
d_{13} δ	1	4.2	7.1	10.0	14.3	20.8	32.3	50.0	70.0	112.9	133.2
	2	4.3	7.3	10.2	14.3	20.0	29.3	42.7	56.5	108.3	133.8
η	1	0.999	0.994	0.987	0.968	0.926	0.813	0.613	0.449	0.412	0.535
	2	0.994	0.981	0.963	0.928	0.861	0.725	0.504	0.311	0.170	0.299
f_{17} δ	1	−0.47	−0.78	−0.94	−1.0	−1.1	−1.1	−1.1	−1.1	−1.0	−1.0
	2	−0.5	−0.8	−0.97	−1.0	−1.0	−1.0	−0.97	−0.97	−0.91	−0.91
η	1	1	1	1	1	1	1	1	1	1	1
	2	1	1	1	1	1	1	1	1	1	1
f_{15} δ	1	0.9	1.7	2.4	3.0	3.5	3.9	4.1	4.2	4.3	4.3
	2	1.1	1.8	2.3	2.8	3.4	4.0	4.6	5.0	5.9	6.7
η	1	1	1	1	1	1	1	1	1	1	1
	2	1	1	1	1	1	1	1	1	1	1

[a] δ = real part of phase shift in degrees; η = absorption parameter.

TABLE IV. Solutions 1 and 2 for states with $T=\frac{3}{2}$.

Energy (MeV)		310	370	410	450	490	533	572	600	650	698
s_{31} δ	1	−20.7	−23.2	−24.5	−25.5	−26.1	−25.9	−23.6	−22.5	−21.3	−19.4
	2	−20.9	−23.5	−24.9	−25.9	−26.5	−26.4	−24.2	−23.0	−21.8	−20.0
η	1	1.0	1.0	1.0	1.0	1.0	1.0	0.982	0.898	0.762	0.624
	2	1.0	1.0	1.0	1.0	1.0	1.0	0.981	0.897	0.759	0.617
p_{33} δ	1	137.4	146.3	150.2	153.2	155.6	157.6	159.2	160.2	161.7	162.9
	2	137.5	146.5	150.4	153.4	155.8	157.8	159.4	160.4	161.9	163.1
η	1	1.0	1.0	1.0	1.0	1.0	1.0	1.0	1.0	1.0	1.0
	2	1.0	1.0	1.0	1.0	1.0	1.0	1.0	1.0	1.0	1.0
p_{31} δ	1	−11.7	−12.7	−13.1	−12.2	−13.4	−13.4	−13.4	−13.5	−13.6	−13.7
	2	−11.4	−12.5	−13.0	−13.3	−13.5	−13.6	−13.8	−13.9	−14.1	−14.5
η	1	0.965	0.937	0.917	0.898	0.879	0.837	0.835	0.818	0.783	0.736
	2	0.972	0.949	0.932	0.916	0.898	0.879	0.860	0.845	0.814	0.773
d_{35} δ	1	−0.3	−0.6	−0.9	−1.3	−1.7	−2.3	−2.7	−3.0	−2.6	−1.1
	2	−0.3	−0.6	−0.8	−1.1	−1.4	−1.9	−2.4	−2.8	−3.7	−4.5
η	1	1.0	1.0	0.998	0.994	0.998	0.974	0.953	0.930	0.880	0.845
	2	1.0	1.0	0.999	0.998	0.996	0.992	0.985	0.977	0.952	0.905
d_{33} δ	1	−1.2	−0.6	−0.5	−0.4	−0.4	−0.3	−0.3	−0.3	−0.3	−0.3
	2	−1.4	−0.7	−0.5	−0.4	−0.4	−0.4	−0.3	−0.3	−0.3	−0.3
η	1	1.0	1.0	1.0	1.0	1.0	1.0	1.0	1.0	1.0	1.0
	2	0.999	1.0	1 0	1 0	1.0	1.0	1.0	1.0	1.0	1.0
f_{37} δ	1	2.8	3.8	3.9	3.9	3.8	3.6	3.4	3.3	3.1	3.0
	2	2.1	3.1	3.5	3.6	3.5	3.4	3.3	3.2	3.1	3.0
f_{35} δ	1	−0.9	−1.0	−1.0	−1.0	−0.9	−0.8	−0.8	−0.7	−0.7	−0.7
	2	−1.3	−1.1	−1.0	−0.9	−0.8	−0.7	−0.7	−0.6	−0.6	−0.6

[a] δ is the real part of the phase shift in degrees; η is the absorption parameter.

C. Goodness of Fit

The χ^2's for the fit of solution 1 to each set of experimental data are given along with the corresponding graphs in Figs. 1–33. (Solution 2 fits the experiments rather better.) These χ^2's are somewhat larger (up to about a factor 2.5) than those obtained in orthodox phase-shift analyses at a *single* energy, which is not surprising since we have a small number of parameters (15 in the π^+ case, 26 in the π^-) to fit the data at *all* energies; our χ^2 are comparable with those obtained by Roper.[4] Nevertheless, the goodness of fit requires some discussion.

In principle, our method of parameterization is

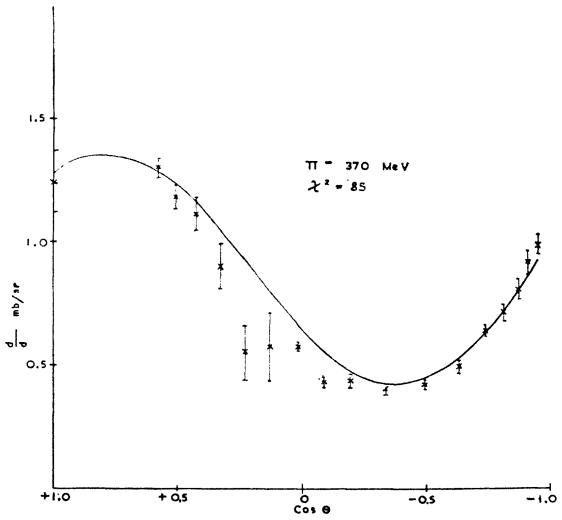

FIG. 13. The fit of solution 1 to the $\pi^{\pm}$-p differential cross section.

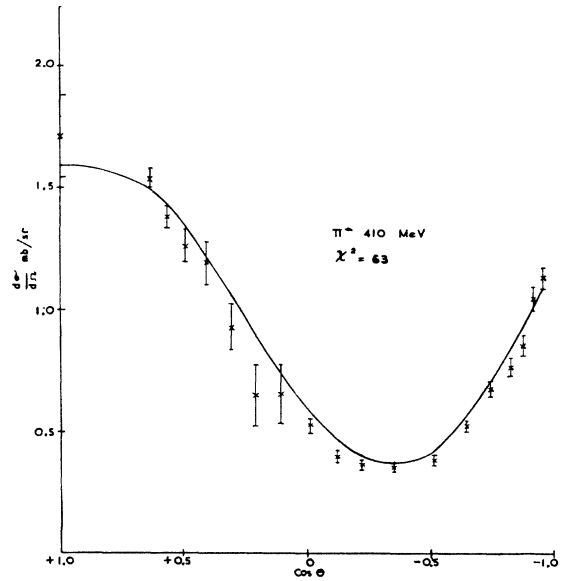

FIG. 14. The fit of solution 1 to the $\pi^{\pm}$-p differential cross section.

capable of reproducing behavior of any degree of complexity; in practice we can only reproduce a reasonably smooth behavior with energy of each partial wave since we are limited by computer speed in our number of parameters. If the partial waves in fact have such a smoothness, then we have here a strong feature of the method, for our parameterization cannot follow even slightly wrong or inconsistent excursions by the experimental data. In that case our larger χ^2 would represent faults in the data such as errors of normalization, assignment of too small "errors," etc. On the other hand, if the physical partial-wave amplitudes are not smooth in their energy dependence, then we must have a larger χ^2 because of our paucity of parameters. In this latter case, however, we would still expect our results to reproduce the grosser features of the amplitudes while ignoring the fine structure.

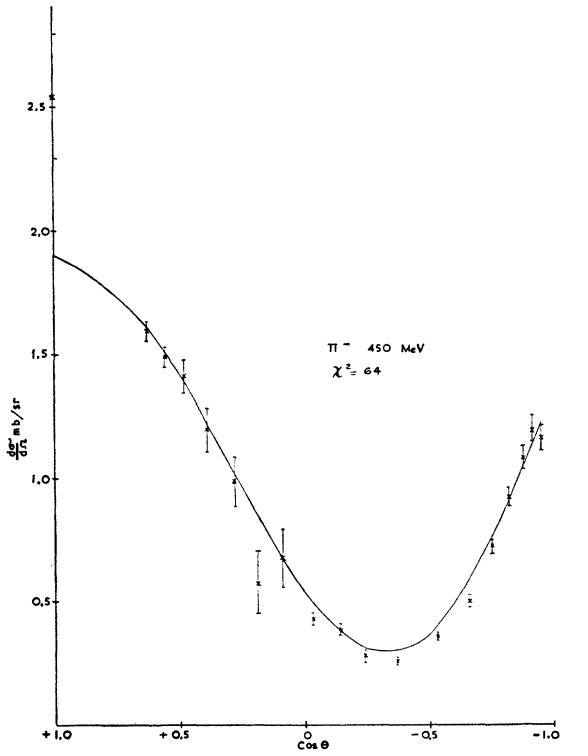

FIG. 15. The fit of solution 1 to the $\pi^{\pm}$-p differential cross section.

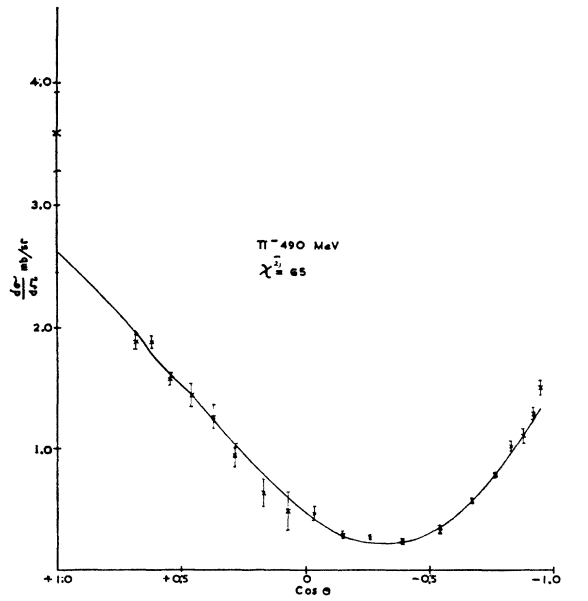

FIG. 16. The fit of solution 1 to the $\pi^{\pm}$-p differential cross section.

7. DISCUSSION AND CONCLUSION

In the neighborhood of the "600-MeV resonance" we obtain three large amplitudes with $T=\frac{1}{2}$ (s_{11}, d_{13}, and p_{11}). In Figs. 38 and 39 we plot $[q\,\mathrm{Im}f(q)]$ versus $[q\,\mathrm{Re}f(q)]$ for these amplitudes in the case of solutions 1 and 2, respectively. In such a complex amplitude diagram, if a certain partial-wave describes an anticlockwise circle with increasing energy, then we say that partial wave has a resonance and we provisionally ascribe the energy at the top of the circle as the resonance energy.[28] The circle may be displaced and even distorted by background, and the smaller the radius of

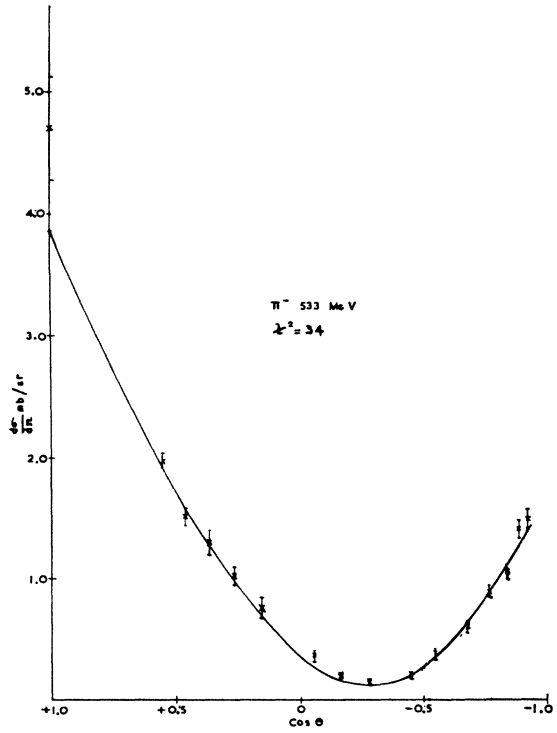

FIG. 17. The fit of solution 1 to the $\pi^{\pm}$-p differential cross section.

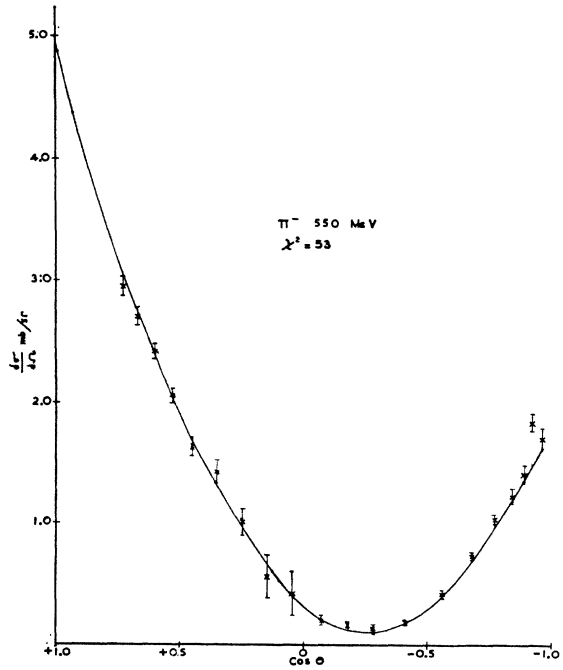

FIG. 18. The fit of solution 1 to the $\pi^{\pm}$-p differential cross section.

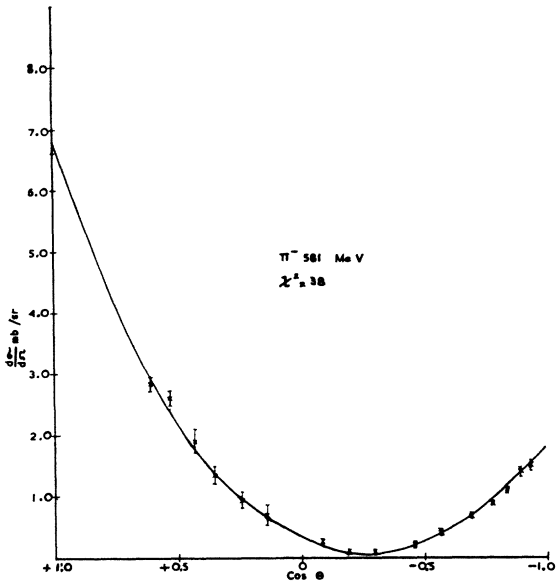

FIG. 19. The fit of solution 1 to the $\pi^{\pm}$-p differential cross section.

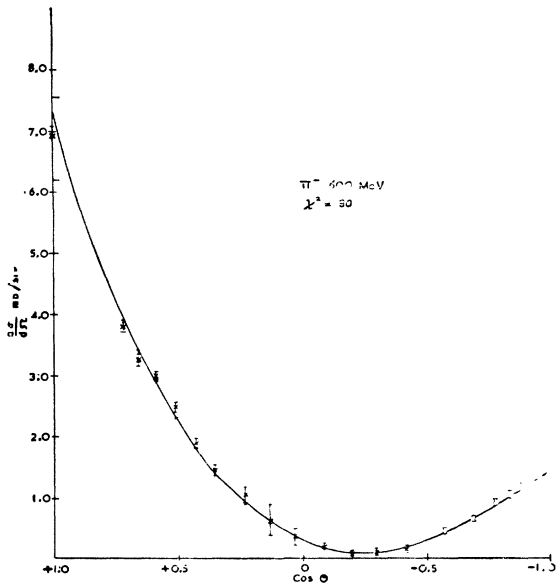

FIG. 20. The fit of solution 1 to the $\pi^{\pm}$-p differential cross section.

[28] See the article by R. H. Dalitz, Ann. Rev. Nucl. Sci. **13**, 346 (1964) for a general discussion of resonant states.

the circle the more inelastic is the resonance. Among other effects of background the resonance position (defined as that energy where the point tracing the circle moves fastest as a function of energy) may be displaced from the top of the circle. A completely elastic resonance is represented by the circle of radius 0.5, center $(0,0.5i)$ which bounds $[qf(q)]$.[29]

The diagrams show, as expected, that both solutions have an inelastic d_{13} resonance. In 1 the resonance energy is 625 MeV with a full width of 170 MeV while

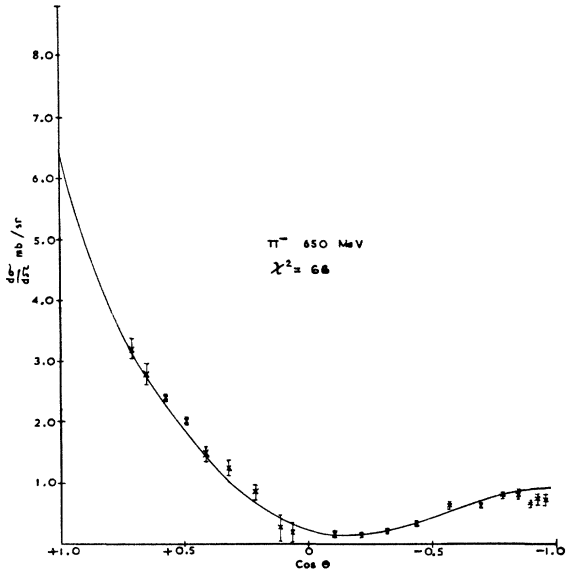

FIG. 21. The fit of solution 1 to the $\pi^{\pm}$-p differential cross section.

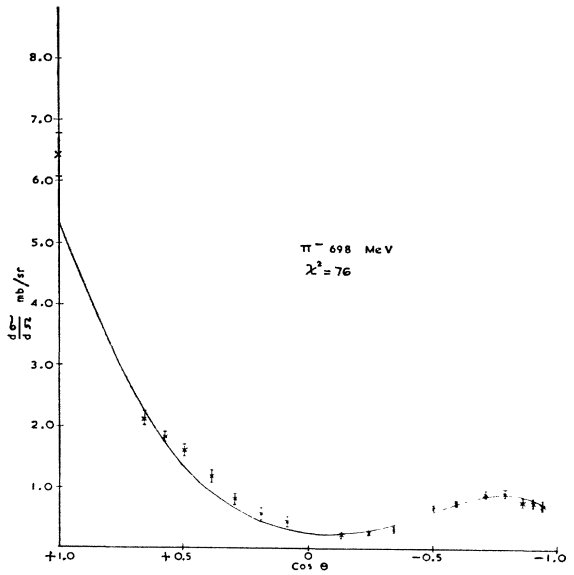

FIG. 22. The fit of solution 1 to the $\pi^{\pm}$-p differential cross section.

[29] If we draw a line from the center of the circle to the amplitude point qf, then the length of this line is η and it makes an angle 2δ with the downward radius.

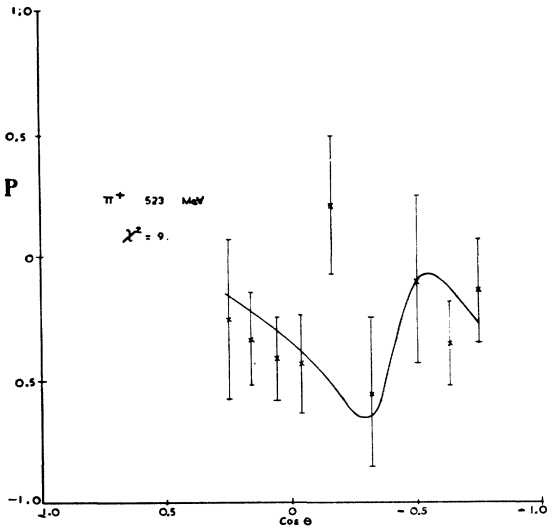

FIG. 23. The fit of solution 1 to the polarization in $\pi^{\pm}$-p scattering.

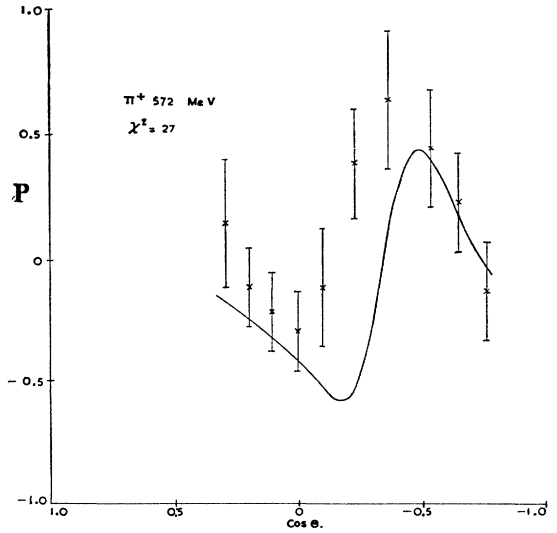

FIG. 24. The fit of solution 1 to the polarization in $\pi^{\pm}$-p scattering.

a more inelastic resonance with resonance energy 630 MeV with a full width of 180 MeV is found in 2.

These correspond to masses and mass widths of

Solution 1: $M=1527$ MeV/c^2, $\Gamma=105$ MeV/c^2.

Solution 2: $M=1530$ MeV/c^2, $\Gamma=111$ MeV/c^2.

The indication is that the mass of this resonance is greater, and the width considerably smaller, than values obtained by inspection of total cross sections.[30] The reason for the unreliability of the estimate from total cross sections is evidently the occurrence of large p_{11} and s_{11} amplitudes.

[30] See, for example, A. H. Rosenfeld *et al.*, University of California Radiation Laboratory Report No. UCRL 8030, 1963 (unpublished).

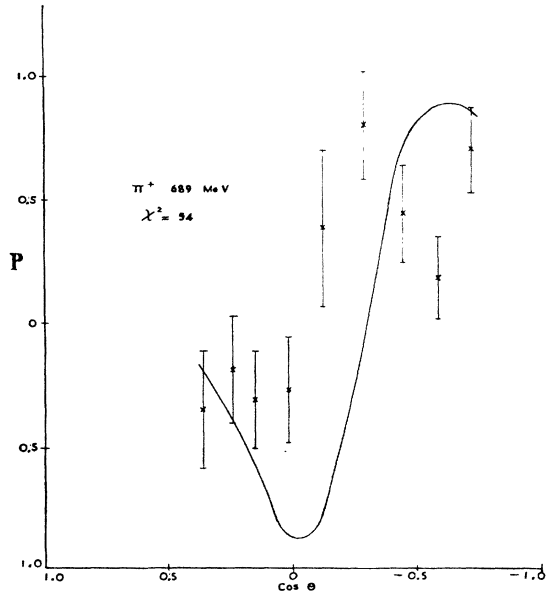

FIG. 25. The fit of solution 1 to the polarization in $\pi^{\pm}$-p scattering.

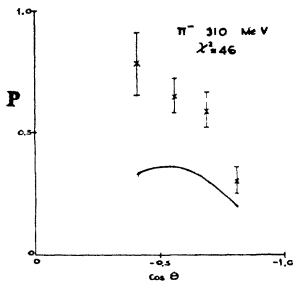

FIG. 26. The fit of solution 1 to the polarization in $\pi^{\pm}$-p scattering.

Both the s_{11} solutions show the η-threshold cusp at 558 MeV; unfortunately, as this cusp is in an s wave in a region where other waves are strongly varying, direct experimental observation of it is almost impossible. The Argand diagrams reveal that, despite δ passing through $\frac{1}{2}\pi$ for the solution 2 s_{11} wave and through 0 for the solution 1 s_{11} wave, the two solutions are qualitatively similar. The circular form is strongly suggestive of resonance (particularly for solution 2) though consideration is complicated by the cusp at the η threshold. It is probably desirable to examine these solutions in a multichannel formalism, using the η-production data,[31] to decide whether or not an s-wave resonance exists.[31a]

The p_{11} amplitude is similar in both solutions and in neither is it easy to interpret. It has some characteristics of a resonance, but the distortion and slowing down of energy variation after 410 MeV make such an identification extremely doubtful. It could be a resonance with fairly rapid variation of background and inelasticity, and if the resonance were placed at the point of fastest energy variation this would be at $T_{\pi}\simeq 380$ or $M\simeq 1370$ MeV/c^2. The inelasticity in this state is probably associated with the reaction

$$\pi+N\rightarrow\pi+\pi+N$$

with the two pions in a relative s state.[32]

In both solutions the d_{15} and f_{15} waves are becoming

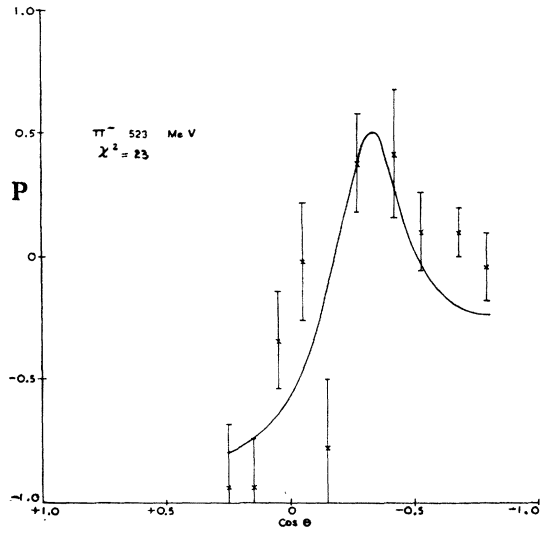

FIG. 27. The fit of solution 1 to the polarization in $\pi^{\pm}$-p scattering.

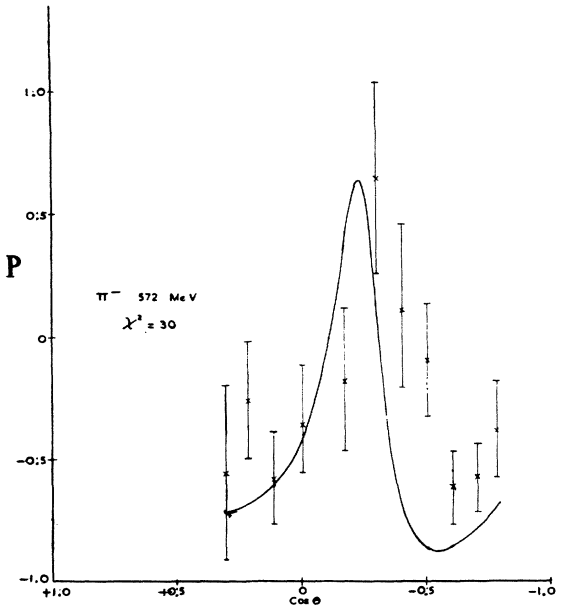

FIG. 28. The fit of solution 1 to the polarization in $\pi^{\pm}$-p scattering.

[31] F. Bulos *et al.* Phys. Rev. Letters **13**, 486 (1964).

[31a] Such an analysis has been carried out by A. W. Hendry and R. G. Moorhouse, Phys. Letters **18**, No. 2 (1965), and it was concluded that such a resonance exists.

[32] M. B. Watson, M. Ferro-Luzzi, and R. D. Tripp, Phys. Rev. **131**, 2248 (1963).

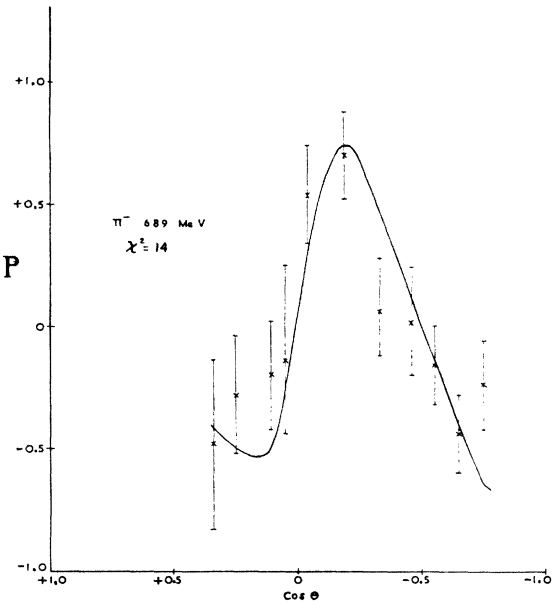

FIG. 29. The fit of solution 1 to the polarization in $\pi^{\pm}$-p scattering.

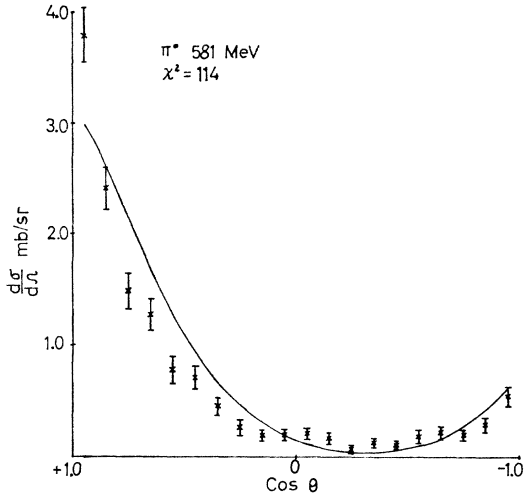

FIG. 30. The fit of solution 1 to pion-nucleon charge-exchange cross sections.

appreciable at 700 MeV, and it is certainly not possible to say for example that the f_{15} will resonate at 900 MeV and the d_{15} will not. Both amplitudes may well be large at 900 MeV; for example, the f_{15} may resonate while the d_{15} amplitude may be large (mainly imaginary) and slowly varying. Such a behavior is compatible with the latest charge-exchange results[33] (which indicate d_{15}-f_{15} interference rather than d_{35}-f_{15} interference) and with the rather rapid rise of our d_{15} phases round 700 MeV.[33a]

There is a good measure of general agreement with the results of the analyses of Roper and Wright[4] and of Auvil *et al.*,[34] the agreement with the latter authors being better. One of the most interesting differences is in the p_{11} wave, the real part δ_{11} of the phase shift for which Roper and Wright find to pass through 90°,

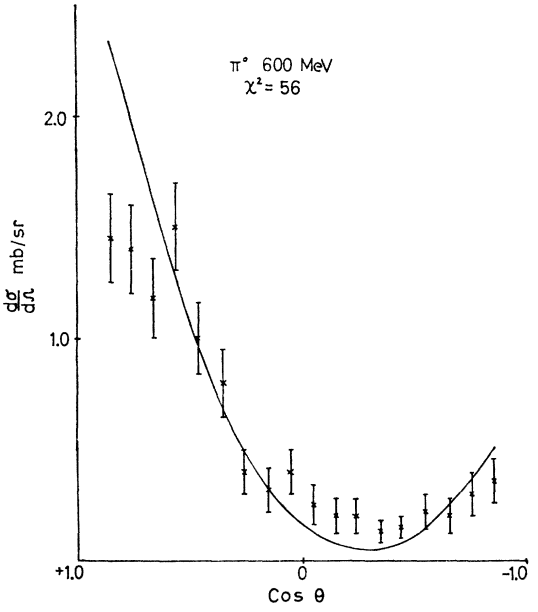

FIG. 31. The fit of solution 1 to pion-nucleon charge-exchange cross sections.

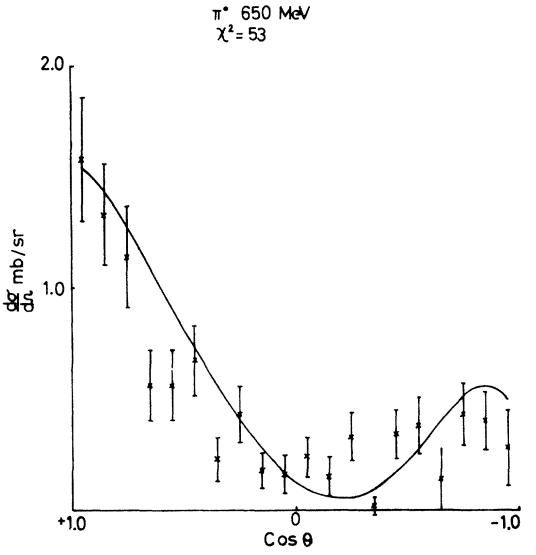

FIG. 32. The fit of solution 1 to pion-nucleon charge-exchange cross sections.

[33] R. J. Cence (private communication); F. Bulos *et al.*, Phys. Rev. Letters **13**, 558 (1964).

[33a] Further differential cross sections and polarizations in the region of 750–1450 MeV are now available; P. J. Duke *et al.* Rutherford Laboratory Report No. RPP/H/8 (unpublished). From inspection of the coefficients of the Legendre expansions, P. G. Murphy (private communication) suggests that both waves are resonant, the d_{15} being very inelastic. Preliminary results of the extension of the work of this paper, by the present authors, confirm this.

[34] P. Auvil, A. Donnachie, A. T. Lea, and C. A. Lovelace, Phys. Letters **12**, 76 (1964).

Auvil *et al.* find to touch 90°–100° and we find not to exceed 70°. However, if one considers the amplitudes, looking at them in the Argand diagram, one sees that these three solutions are not very dissimilar.[35] The reason is that for $T_\pi > 500$ MeV the absorption parameter η_{11} is very small and thus small changes in the amplitude can lead to large changes in δ_{11}. Additionally it is in this region that the p_{11} amplitude of Auvil *et al.* is least well determined.[34] When these authors make a fit to their solution using dispersion relations, they find that the resulting δ_{11} does not now reach 90° and that their solution approaches quite closely to the p_{11} solutions of this paper.[36]

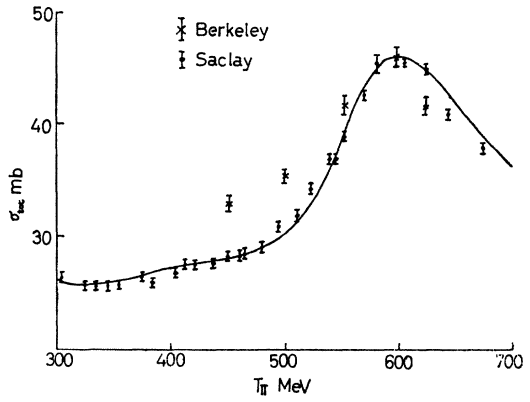

FIG. 33. Comparison of solution 1 with the Saclay (Ref. 21) (solid circles) and Berkeley (Ref. 11) (crosses) $\pi^- p$ total scattering cross sections.

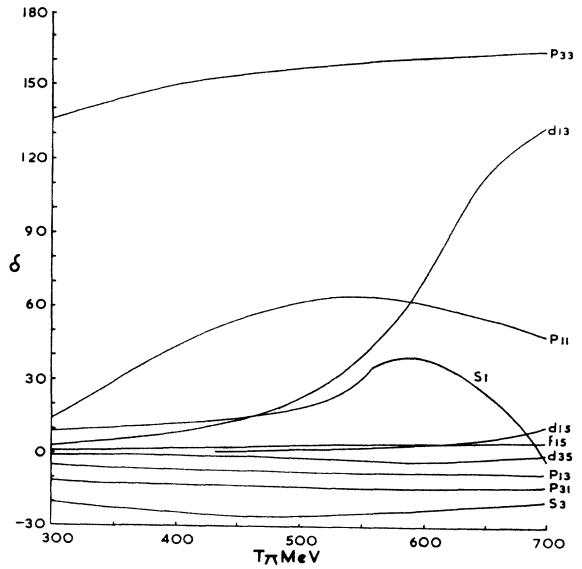

FIG. 34. The real part of the phase shifts δ for the larger amplitudes of solutions 1.

[35] R. H. Dalitz and R. G. Moorhouse, Phys. Letters 14, 159 (1965).
[36] A. Donnachie, A. T. Lea, and C. Lovelace, Proc. Roy. Soc. (London) (to be published).

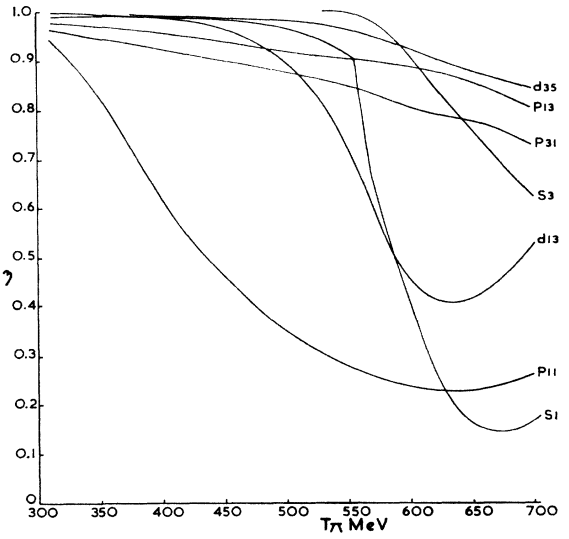

FIG. 35. The absorption parameters η of solution 1.

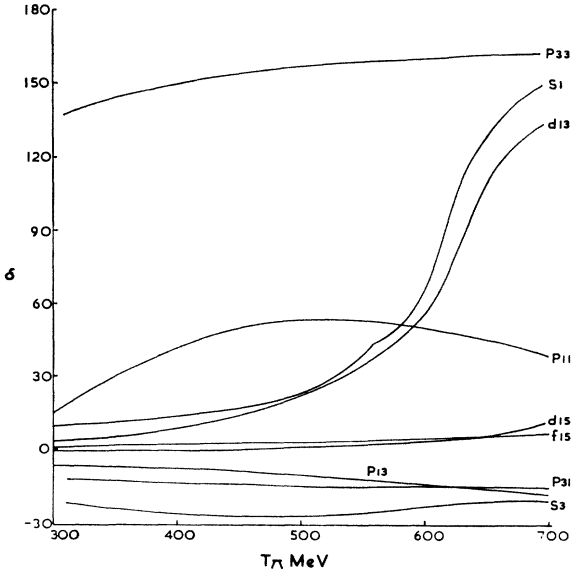

FIG. 36. The real part of the phase shifts δ for the larger amplitudes of solution 2.

It is intended to carry out further investigations in the πN system with this method of partial wave analysis. The possibility, however unlikely, of a p_{13} resonance (rather than d_{13}) at 600 MeV has not been fully explored and searches with a more general parameterization of the p_{11} inelasticity are probably also desirable.

These and further refinements are probably best carried out in conjunction with an extension of the energy range up to the "fourth resonance" from 300 to 1400-MeV pion laboratory energy. Further experimental results of differential cross sections, including charge exchange, and polarization are becoming available in the range 700–1400 MeV.

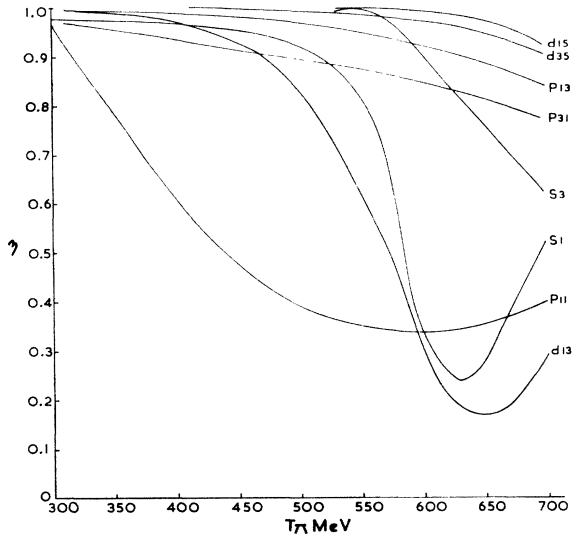

FIG. 37. The absorption parameters η of solution 2.

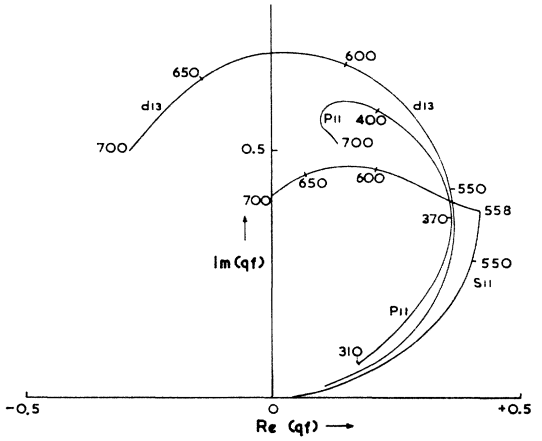

FIG. 38. The Argand diagram of $qf=(1/2i)(\eta e^{2i\delta}-1)$ for the s_{11}, p_{11}, and d_{13} amplitudes of solution 1.

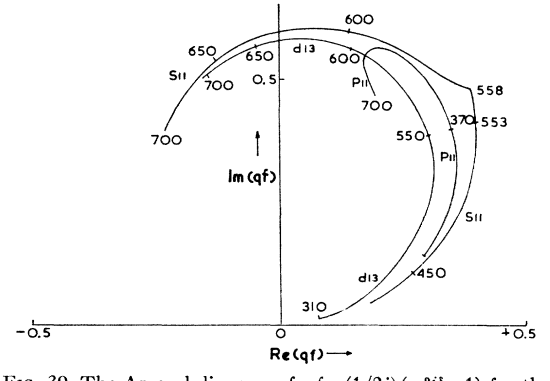

FIG. 39. The Argand diagram of $qf=(1/2i)(\eta e^{2i\delta}-1)$ for the s_{11}, p_{11}, and d_{13} amplitudes of solution 2.

ACKNOWLEDGMENTS

The authors would like to express their gratitude to the Director and staff of the Deutsches-Rechenzentrum, Darmstadt for their generous assistance in providing computing and other facilities.

APPENDIX A

We list here references to all data considered for our analysis. The type of data given in each reference is indicated by the appropriate symbol (defined below) and numbers given in brackets give the energy at which the observation was made.

Symbols used. We use the following: π^+, π^-, and π^0 indicate that the reference gives results of π^+p, π^-p, and charge-exchange differential cross sections; a subscript "T" denotes total cross sections, subscript "el" denotes total elastic cross section, and a suffix "p" denotes polarization measurements of the outgoing nucleon. Thus, $\pi_T{}^-(310)$ would indicate that a measurement was made at 310 MeV of the total cross section for the scattering of negative pions on protons.

A1. H. L. Anderson, E. Fermi, R. Martin, and D. E. Nagle, Phys. Rev. **91**, 155 (1953). π^+ at 78, 110, 135 MeV.

A2. H. L. Anderson and M. Glicksman, Phys. Rev. **120**, 268 (1955). π^+, $\pi_T{}^+$ at 165 MeV.

A3. H. L. Anderson, W. C. Davidson, M. Glicksman, and U. E. Kruse, Phys. Rev. **100**, 279 (1955). π^+ and $\pi_T{}^+$ at 189 MeV.

A4. J. Ashkin, J. P. Blaser, F. Feiner, and M. O. Stern, Phys. Rev. **105**, 724 (1957). π^+ and $\pi_T{}^+$ at 220 MeV.

A5. J. Ashkin, J. P. Blaser, F. Feiner, and M. O. Stern, Phys. Rev. **101**, 1149 (1956). π^+ at 150 and 170 MeV.

A6. P. Bareyre, C. Bricman, G. Valladas, G. Villet, J. Bizard, and J. Sequinot, Phys. Letters **8**, 137 (1964). $\pi_T{}^-$ in the range 300 to 700 MeV.

A7. F. Bulos, R. E. Lanou, A. E. Pifer, A. M. Shapiro, M. Widgoff, R. Panvini, A. E. Brenner, C. A. Bordner, M. E. Law, E. E. Ronat, K. Strauch, J. Szynansky, P. Bastien, B. B. Brabson, Y. Eisenberg, B. T. Feld, V. K. Fischer, I. A, Pless, L. Rosenson, R. K. Yamamoto, Cz. Calvelli, L. Guerririo, Cz. A. Salandin, A. Tomasin, L. Ventura, C. Vico, and F. Waldner, Phys. Rev. Letters **13**, 558 (1964). π^0, $\pi_T{}^0$, 545, 588, 619, 659, and 755 MeV.

A8. R. J. Cence (private communication). π^0.

A9. T. J. Devlin, R. W. Kenney, P. G. McManigal, and B. J. Moyer, Phys. Rev. **136**, B356 (1964); **136**, B1187 (1964). $\pi_p{}^+$, $\pi_p{}^-$ at 523, 572, 689 MeV.

A10. L. K. Goodwin, R. W. Kenney, and V. Perez-Mendez, Phys. Rev. **122**, 655 (1961). π^- at 370 and 427 MeV.

A11. J. A. Helland, T. J. Devlin, D. E. Hagge, M. J. Longo, B. J. Moyer, and C. D. Wood, Phys. Rev. Letters **10**, 27 (1963). π^+, $\pi_T{}^+$, π^-, $\pi_T{}^+$ at 533, 581, and 698 MeV.

A12. S. J. Lindenbaum and L. C. L. Yuan, Phys. Rev. **100**, 306 (1955). $\pi_T{}^+$ at 146, 157, 166, 171, 173, 181, 189, 214, 222, 262, 263, 298, and 335 MeV. Phys. Rev. **111**, 1380 (1958). $\pi_T{}^+$ at 143, 162, 170, 173, 177, 183, 195, and 205 MeV.

A13. A. E. Muklin, E. B. Ozerov, and B. M. Pontecorvo, Zh. Eksperim. i Teor. Fiz. **31**, 371 (1956) [English transl.: Soviet Phys.—JETP **4**, 237 (1957)].

A14. A. Muller, E. Pauli, R. Barloutand, J. Meyer, M. Beneventano, G. Gialanella, and L. Paoluzzi, Phys. Letters **10**, 349 (1964). π^0 at 600, 650, and 728 MeV.

A15. P. M. Ogden, University of California Report No. UCRL-11180 (unpublished), π^+ at 370, 410, 450, 490, 550, 600, and 650 MeV. π^- at 370, 410, 450, 490, 550, 600, and 650 MeV.

A16. E. H. Rogers, O. Chamberlain, J. Foote, H. Steiner, C. Wiegand, and T. Ypsilantis, Rev. Mod. Phys. **33**, 356 (1961). π^+, $\pi_p{}^+$ at 310 MeV.

A17. H. R. Rugge and O. T. Vik, Phys. Rev. **129**, 2300 (1963). π^-, $\pi_p{}^-$ at 310 MeV.

A18. H. D. Taft, Phys. Rev. **101**, 1116 (1956). $\pi_T{}^+$ at 217 MeV.

A19. I. M. Vaselevskii and V. V. Vishnyckov, Zh. Eksperim. i Teor. Fiz. **38**, 1644 (1960) [English transl.: Soviet Phys.—JETP **11**, 1185 (1960)]. $\pi_p{}^-$ at 300 MeV. Zh. Eksperim. i Teor. Fiz. **38**, 441 (1960) [English transl.: Soviet Phys.—JETP **11**, 323 (1960)]. π^- at 300 MeV.

A20. V. G. Zinov and S. M. Korenchenko, Zh. Eksperim. i Teor. Fiz. **38**, 1099 (1960) [English transl.: Soviet Phys.—JETP **11**, 794 (1960)]. π^- at 307 and 333 MeV.

APPENDIX B

The following expressions for the real and imaginary parts of the inverse partial-wave scattering amplitude are those used in the computer program:

$$\mathrm{Im}f_{l\pm}^{-1}=-qR_{l\pm}(q)\,, \tag{B1}$$

$$\mathrm{Re}f_{l\pm}^{-1}=-\frac{(q^2-q_0^2)}{\pi}\int_0^Q dx^2\frac{xR_{l\pm}(x)}{(x^2-q^2)(x^2-q_0^2)}-\frac{1}{\pi}\sum\frac{d_{l\pm}{}^m}{q^2+q_m{}^2}+\sum_{n=0}^{l}\frac{\lambda_n}{q^{2n}}\,, \tag{B2}$$

where

$$R_{l\pm}(q)=1+\theta(q-q_1)\left\{a_{l\pm}\frac{q(q-q_1)}{(1+q^2/A^2)}+b_{l\pm}\frac{(q-q_1)}{(1+q^2/B^2)}\right\}+\theta(q-q_1)\left\{c_{l\pm}\frac{q(q-q_2)}{(1+q^2/C^2)}+\delta_{l,0}d_{l\pm}\frac{q(q^2-q_2^2)^{1/2}}{(1+q^2/D^2)}\right\}. \tag{B3}$$

Equation (B2) is a modified form of Eq. (3.2). The second (left-hand-cut) integral of (3.2) is evaluated by approximating $\Delta f_{l\pm}^{-1}$ by a sum of poles (3.7) and absorbing part of the integral in λ_0. In the first (right-hand-cut) integral of (3.2) the upper limit of x^2 has been replaced by a finite cutoff Q, where Q is larger than any center-of-mass momentum in the energy range to be analyzed, as explained in Sec. 3.

Define

$$I_{l\pm}(q^2,q_0^2,Q)=-\frac{(q^2-q_0^2)}{\pi}\int_0^Q dx^2\frac{xR_{\pm}(x)}{(x^2-q^2)(x^2-q_0^2)}\,.$$

The forms of (B2) (for each partial wave) that were actually used in the computer program are as follows:

$$s_{31}\colon\ \mathrm{Re}f_{0+}^{-1}(q)=I_0(q^2,q_0^2,Q)-I_{0+}(0,q_0^2,Q)+\lambda_0+\left\{\frac{d_1}{(q^2+1+|a_1|)}-\frac{d_1}{(1+|a_1|)}\right\}+\frac{d_2q^2(q^2-q_1^2)}{(q^2+1+|a_2|)}\,; \tag{B4}$$

$$\left.\begin{aligned} s_{11}\colon\ \mathrm{Re}f_{0+}^{-1}(q)&=I_{0+}(q^2,q_0^2,Q)-I_{0+}(0,q_0^2,Q)+\lambda_0+\frac{d_1q^2}{1+q^2}+\frac{d_2q^2(q^2-b_1)(q^2-b_2)}{(q^2+|a_1|)(q^2+|a_2|)(q^2+|a_3|)}\,;\\ p_{33}\colon\ \mathrm{Re}f_{1+}^{-1}(q)&=I_{1+}(q^2,q_0^2,Q)+\lambda_0+\frac{\lambda_1}{q^2}+\frac{d_1}{(q^2+1+|a_1|)}+\frac{d_2(q^2-2.8157)}{(q^2+1+|a_2|)}\,; \end{aligned}\right\} \tag{B5}$$

$$p_{31},\,p_{13}\colon\ \mathrm{Re}f_{1\pm}^{-1}(q)=I_{1\pm}(q^2,q_0^2,Q)+\lambda_0+\frac{\lambda_1}{q^2}+\frac{d_1}{(q^2+1+|a_1|)}+d_2(q^2-4.23)/(q^2+|a_2|)\,; \tag{B6}$$

$$p_{11}\colon\ \mathrm{Re}f_{1-}^{-1}(q)=F(q^2)-F(-q_m^2)\frac{(q^2+q_m^2)}{(q^2-3.0)}\,; \tag{B7}$$

where

$$F(q)=I_{1-}(q^2,q_0^2,Q)+\lambda_0+\frac{\lambda_1}{q^2}+\frac{d_1(q^2-b_1)}{(q^2+1+|a_1|)}\,. \tag{B8}$$

This is a special form which, by means of the pole in $\mathrm{Re}f^{-1}$, ensures that the p_{11} amplitude has a zero at 200 MeV.

d and f amplitudes:

$$\mathrm{Re}f_{l\pm}^{-1}=I_{l\pm}(q^2,q_0^2,Q)+\frac{\lambda_2}{q^4}+\frac{\lambda_2}{q^6}+\frac{d_1}{(q^2+1+|a_1|)}+\frac{d_2(q^2-4.23)}{(q^2+1+|a_2|)}\,.$$

The units in (B4)–(B8) are pion-mass units. When the maximum power of q^2 in a numerator is greater than or equal to the maximum power in the corresponding denominator, as in (B5), it may appear that we have departed from our prescription of poles on the left-hand cut. However, for the energy range 300–700 MeV considered $q^2<13$, so that the situation is in fact that of the quite harmless approximation of putting distant poles at infinity.

The various quantities, such as λ_0, $\lambda_1\cdots$, are different in each partial wave. The computer program contains a subprogram which expresses the quantities above in terms of the parameters x_1, x_2, $\cdots$ which are actually varied in the search for a minimum. We now give the actual expressions for these quantities which were used in the search leading to solution 1.

$T=\frac{3}{2}$ Parameterization.

$$\begin{aligned} s_{31}\colon\ & a=0.25|x_9|/(1+|x_9|)\,;\quad b=0\,;\quad c=2|x_8|/(1+|x_8|)\,;\\ & \lambda_0=-11.36\,;\quad d_1=-9.04+4x_{14}/(1+|x_{14}|)\,;\\ & a_1=0.283\,;\quad d_1=x_1/(1+|x_1|)\,;\quad a_2=20\,. \end{aligned}$$

p_{33}: $a=0$; $b=0$; $c=2(x_{10})^3/(1+|x_{10}|^3)$;
$\lambda_0=-1142$; $\lambda_1=4.65$; $d_1=1\,579\,000$
$a_1=1381$; $d_2=1.8x_3/(1+|x_3|)$; $a_3=20$.

p_{31}: $a=0.5|x_{11}|/(1+|x_{11}|)$; $b=0$; $c=0$;
$\lambda_0=3x_{15}/(1+|x_{15}|)$; $\lambda_1=-26.32$; $d_1=-20$;
$a_1=0.0025$; $d_2=100x_2/(1+|x_2|)$; $a_2=20$.

d_{35}: $a=4+3x_{12}/(1+|x_{12}|)$; $b=0$; $c=0$;
$\lambda_2=-10\,000$; $\lambda_3=0$; $d_1=700+300x_4/(1+|x_4|)$;
$a_1=0$; $d_2=0$; $a_2=20$.

d_{33}: $a=0.4|x_{14}|/(1+|x_{14}|)$; $b=0$; $c=0$;
$\lambda_2=-1000$; $\lambda_3=0$;
$d_1=0$; $a_1=0$; $d_2=3000x_5/(1+|x_5|)$; $a_2=20$.

f_{37}: $a=b=c=0$;
$\lambda_2=0$; $\lambda_3=4098$;
$d_1=0$; $a_1=0$; $d_2=400|x_6|/(1+|x_6|)$; $a_2=20$.

f_{35}: $a=b=c=0$;
$\lambda_2=0$; $\lambda_3=-12210$;
$d_1=0$; $a_1=0$; $d_2=-1500|x_7|/(1+|x_7|)$.

$T=\frac{1}{2}$ *Parameterization.*

s_{11}: $a=0.25|x_{19}|/(1+|x_{19}|)$; $b=0$; $c=0$; $d=|x_{10}|/(1+|x_{10}|)$;
$\lambda_0=5.58$; $d_1=5.63(1+0.8x_{15}/(1+|x_{15}|)$;
$d_2=4000+8000x_1/(1+|x_1|)$; $b_1=4.23$; $b_2=2.0+0.8x_{16}/(1+|x_{16}|)$;
$a_1=21.0$; $a_2=41.0$.

p_{13}: $a=3|x_{14}|/(1+|x_{14}|)$; $b=0$; $c=0$;
$\lambda_0=-21.94+18.0x_5/(1.0+|x_5|)$; $\lambda_1=-34.48$;
$d_1=0$; $a_1=0$; $d_2=-30.0+180.0x_6/(1+|x_6|)$; $a_2=21.0$;

p_{11}: $a=0.30|x_{11}|/(1+|x_{11}|)$; $b=4.0|x_{12}|/(1+|x_{12}|)$; $c=0$;
$\lambda_0=7.0x_2/(1.0+x_2)$; $\lambda_1=-9.9$;
$d_1=-4.0+8.0x_3/(1.0+|x_3|)$; $b_1=4.23$; $a_1=20.0$;
$q_m=1.41$.

d_{15}: $a=0.25|x_{18}|/(1.0+|x_{18}|)$; $b=0$; $c=|x_{26}|/(1+|x_{26}|)$;
$\lambda_2=9296.0+929.6x_{20}/(1.0+x_{20})$; $\lambda_3=0$;
$d_1=0$; $d_2=250.0+500.0x_7/(1+|x_7|)$; $a_2=20.0$.

d_{13}: $a=0.075+0.075x_{13}/(1.0+|x_{13}|)$; $b=0$; $c=0$;
$\lambda_2=403.8+40.38x_{21}/(1.0+|x_{21}|)$; $\lambda_3=0$;
$d_1=50.0+30.0x_4/(1.0+|x_4|)$; $a_1=0$;
$d_2=-18.91-0.445d_1+7.0x_{17}/(1.0+|x_{17}|)$; $a_2=20.0$.

f_{17}: $a=0$; $b=0$; $c=|x_{24}|/(1+|x_{24}|)$;
$\lambda_3=-18830.0+15064.0x_{22}/(1.0+|x_{22}|)$; $\lambda_2=0$;
$d_1=1500.0x_9/(1.0+|x_9|)$; $a_1=0.0$; $d_2=0$.

f_{15}: $a=0$; $b=0$; $c=|x_{25}|/(1+|x_{25}|)$;
$\lambda_2=0$; $\lambda_3=7324.0+7032.0x_{23}/(1.0+|x_{23}|)$;
$d_1=280.0+120.0x_8/(1+|x_8|)$; $a_1=0$; $d_2=0$.

Also $A=7.194$; $B=2.878$; $C=10.791$; $D=10.791$; $q_0=1.0$; $Q=3.8$, $q_1=1.53$, $q_2=3.09$.

The searches were conducted in x space. We give here the values of x at the minimum corresponding to solution 1:

$T=\frac{3}{2}$

$(x_1,x_2,\cdots,x_{15})=$ (0.0028, −0.5702, −0.8609, −0.3477, −65.99, −2.006, 3.808, 1.273,
−0.0006, 0.002, 2.181, −2.000, −0.0027, −0.1892, 0.4965).

$T=\frac{1}{2}$

$(x_1,x_2,\cdots,x_{26})=$ (−2.9421, −0.1669, 2.7053, 14.343, 2.0110, 0.0094, −5.2662, −101170.0, 0.9705, 0.2981,
0.3545, 0.1310, 0.3080, 0.2505, 10.355, −131490.0, 440.0, 0.0003, 0.1682, 0.0913, −1.1633,
−1.0500, 11.7100, 33440.0, 0.0000, 0.0000).